

2M 11.2906.5

Université de Montréal

Diffusion thermique des rayons X sur un modèle de cristal
liquide en colonnes

par

Alexandre Lacombe

Département de Physique

Faculté des Arts et des Sciences

Mémoire présenté à la Faculté des études supérieures
en vue de l'obtention du grade de
Maître ès sciences (M.Sc.)

en physique

Mai 2001



© Alexandre Lacombe, 2001

QC
3
N54
2001
N.012

Université de Montréal
Faculté des études supérieures

Ce mémoire intitulé :

Diffusion thermique des rayons X sur un modèle de cristal
liquide en colonnes

présenté par :

Alexandre Lacombe

a été évalué par un jury composé des personnes suivantes :

Yves Lépine, président-rapporteur
Alain Caillé, directeur de recherche
Sjoerd Roorda, membre du jury

Mémoire accepté le :

*Si les savants cherchent, c'est qu'ils n'ont pas trouvé ;
S'ils n'ont pas trouvé, c'est qu'ils ne savent pas ;
S'ils ne savent pas, ce ne sont donc pas des savants.*

Marc Favreau

SOMMAIRE

Ce mémoire par article traite de la diffusion thermique des rayons X par un cristal liquide en colonnes dans sa phase hélicoïdale ordonnée. Un modèle tri-dimensionnel simplifié du cristal liquide en colonnes, formé de cylindres de densité continue placés sur un réseau triangulaire, est utilisé. Les fonctions de corrélation des fluctuations positionnelles et orientationnelles et les fonctions de corrélation de densité-densité qui sont associées à ce modèle sont calculées à l'aide d'une expression diagonalisée de l'énergie élastique totale. Ces calculs indiquent un quasi-ordre à la fois des fluctuations de position et des fluctuations angulaires de la densité le long des colonnes. En conséquence, les maxima de Bragg, prédicts par le modèle, possèdent des décroissances en lois de puissance fortement anisotropes. Celles-ci ont été calculées, dans l'espace réciproque, aux positions correspondant aux vecteurs du réseau réciproque de même qu'aux positions correspondant à l'orientation périodique de la densité. Enfin, les calculs montrent la persistance de l'ordre à longue portée d'une variable composée de deux quantités qui ne possèdent individuellement qu'un quasi-ordre. Les détails de ces calculs se trouvent dans l'annexe de l'article présenté dans ce mémoire.

TABLE DES MATIÈRES

SOMMAIRE	i
INTRODUCTION	1
OBJECTIF DU TRAVAIL	7
THERMAL DIFFUSE X-RAY SCATTERING IN A MODEL COLUMNAR LIQUID CRYSTAL	8
CONCLUSION	51
ANNEXE : Définition des constantes d'élasticité et de courbure . .	54
CONTRIBUTION DE L'AUTEUR À L'ARTICLE	56
REMERCIEMENTS	57

INTRODUCTION

Le terme *cristal liquide* fait référence à plusieurs états distincts de la matière molle qui possèdent des propriétés structurales intermédiaires entre celles des liquides et des solides¹. En particulier, certains matériaux organiques subissent de nombreuses transitions de phase entre leurs états liquide et solide. Ces phases intermédiaires sont appelées phases mésomorphes (ou mésophases) et présentent des propriétés mécaniques et des symétries intermédiaires entre celles d'un liquide et celles d'un solide cristallin².

Plus spécifiquement, un cristal liquide est un système au sein duquel un ordre semblable à celui présent dans un liquide existe dans au moins une direction de l'espace et qui présente un certain degré d'anisotropie, c'est-à-dire une fonction de corrélation densité-densité $\langle \rho(\vec{r})\rho(\vec{r}') \rangle$ qui ne dépend pas seulement du module $|\vec{r} - \vec{r}'|$ mais aussi de l'orientation de $\vec{r} - \vec{r}'$ par rapport aux axes macroscopiques x , y et z .

Ainsi, on peut obtenir un cristal liquide soit en imposant à ses molécules constituantes un ordre positionnel dans une ou deux dimensions spatiales (ou encore aucun ordre positionnel), soit en assignant à ces mêmes molécules, qui ne possèdent généralement pas de symétrie sphérique, des degrés de liberté orientationnels. On distingue alors les trois types de cristaux liquides suivants :

1. Les nématiques

Les nématiques sont caractérisés par l'absence d'ordre positionnel à longue portée de leurs molécules constituantes, à l'instar des liquides. Cependant, leurs molécules, qui se présentent sous la forme de bâtonnets, possèdent un ordre orientationnel : elles ont en effet une tendance à s'aligner suivant une direction particulière que l'on représente par un vecteur unitaire \hat{n} appelé

¹J. D. Litster et R. J. Birgeneau, *Phases and phase transitions*, Physics Today, mai 1982.

²P.-G. de Gennes et J. Prost, *The physics of liquid crystals*, 2nd Ed., Oxford University Press, New York, 1993.

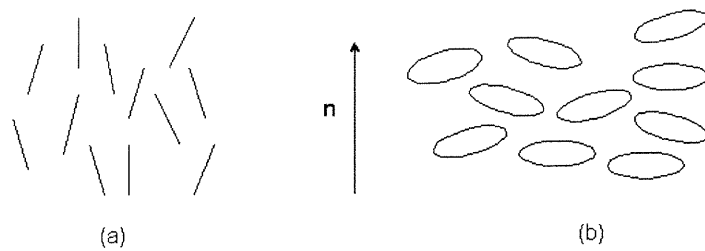


FIG. 1 – Arrangement des molécules dans un nématique (a) fait de molécules en forme de bâtonnets et (b) fait de molécules discoïdes. Les vecteur directeur \hat{n} est illustré.

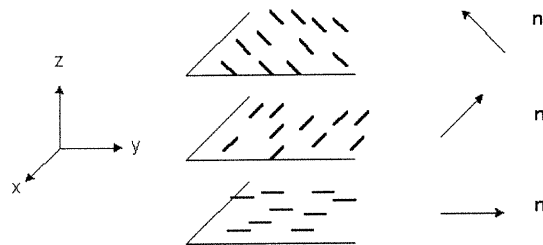


FIG. 2 – Structure des molécules au sein d'un cristal liquide de type cholestérique. On remarque que celles-ci s'orientent suivant un vecteur directeur qui tourne régulièrement autour de l'axe z .

le vecteur directeur. En conséquence, on y observe deux longueurs de corrélation distinctes ξ_{\parallel} et ξ_{\perp} (respectivement parallèle et perpendiculaire à un plan macroscopique prédéfini). La figure 1 illustre schématiquement un tel système.

Il est à noter qu'un nématique peut exister dans une phase dite hélicoïdale (ou chirale, en raison de l'inversion de son image miroir), caractérisée par la rotation régulière du vecteur directeur \hat{n} le long d'un axe donné (voir Fig. 2). Un tel cristal liquide nématique porte le nom de cholestérique. Cette rotation possède le long de l'axe une période spatiale fixe nommée *pitch*.

2. Les smectiques

Ce type de cristal liquide présente un ordre positionnel particulier dans

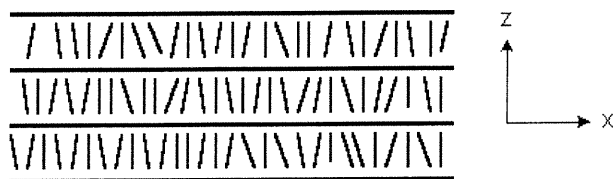


FIG. 3 – La structure moléculaire en couches dans un smectique A.

une direction spatiale seulement. Comme l'a montré A. Caillé³, il s'agit en fait d'un quasi-ordre, une situation caractérisée par une divergence logarithmique de la valeur quadratique moyenne des fluctuations positionnelles des molécules dans cette direction, c'est-à-dire une instabilité de Landau-Peierls. En conséquence, les habituels pics de Bragg sont transformés en maxima de Bragg dont les décroissances en lois de puissance prédictes par A. Caillé ont été observées au M.I.T.⁴

On peut voir un smectique comme un ensemble de couches liquides bidimensionnelles superposées à intervalles réguliers, du moins sur des distances relativement faibles (voir Fig. 3). On connaît aujourd'hui de nombreux types de smectiques, dont les principaux sont les smectiques A, les smectiques C et les smectiques hexatiques.

Les smectiques A ont un arrangement moléculaire du type de celui présenté à la figure 3, c'est-à-dire une structure en couches dont l'épaisseur varie d'une longueur moléculaire à plusieurs milliers d'Ångströms et au sein desquelles les molécules ne possèdent pas d'ordre positionnel à longue portée. Il s'agit conséquemment d'un matériau uniaxial.

Les smectiques C, quant à eux, se présentent aussi en couches bidimensionnelles liquides, mais les molécules qui forment ces couches, si elles ne possèdent toujours pas d'ordre positionnel à longue portée, présentent cependant un ordre orientationnel : elles s'alignent préféablement suivant un

³Caillé, A. C.R. Acad. Sci., Paris **B274**, 891 (1972).

⁴Als-Nielsen, J., Birgeneau, R. J., Kaplan, M., Litster, J. D., et Safinya, C. R., Phys.

Rev. Lett. **39**, 352 (1977) ; **E41**, 1626 (1978) ; **39**, 1668 (1977).

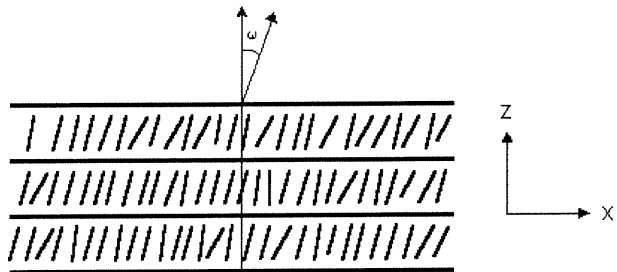


FIG. 4 – Les molécules constitutantes d'un cristal liquide de type smectique C sont en moyenne inclinées d'un angle ω par rapport à l'axe z .

axe qui fait un angle ω avec la direction perpendiculaire à ces couches (voir Fig. 4), ce qui en fait un matériau biaxial. Notons également que le smectique C peut se retrouver dans une phase chirale, notée C*, dans laquelle l'axe d'inclinaison fait une rotation régulière autour de l'axe perpendiculaire au plan des couches (voir Fig. 5).

Enfin, les smectiques hexatiques sont formés de couches liquides bidimensionnelles superposées dont les molécules sont distribuées localement sur un réseau triangulaire. Cependant, en raison du grand nombre de défauts présents dans les couches de ces smectiques, cet ordre positionnel décroît très rapidement, même si la structure triangulaire de base se retrouve sur des distances macroscopiques.

3. Les cristaux liquides en colonnes

Ce type de cristal liquide possède un ordre à longue portée en deux dimensions. On peut le représenter comme un réseau hexagonal bidimensionnel de colonnes "liquides" (voir Fig. 6). On note cet état de la matière D_h , où D signifie *discoïde* (qui est la forme habituelle des molécules constituantes de ces cristaux liquides) et h , *hexagonal*. On rajoute habituellement à ce symbole un second indice qui fait référence au type d'ordre présent au sein des colonnes de molécules. Ainsi, la phase D_{hd} représente un cristal liquide en colonnes désordonnées (où les molécules se comportent réellement comme celles d'un liquide), et la phase D_{ho} représente un cristal liquide en colonnes

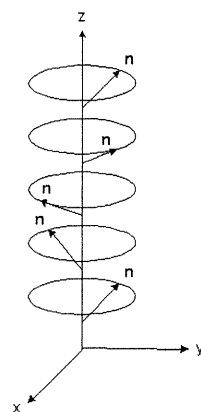


FIG. 5 -- Dans sa phase chirale, le smectique C présente des couches successives de molécules orientées suivant un vecteur directeur qui tourne régulièrement autour de l'axe perpendiculaire à ces couches. Cette phase est notée C*.

"ordonnées", c'est-à-dire dont les molécules sont pourvues d'un certain ordre positionnel le long de l'axe des colonnes.

À l'aide de l'expression de l'énergie libre pour une telle structure et du théorème d'équipartition, on peut facilement montrer qu'en l'absence de résistance au glissement des colonnes les unes sur les autres, le type d'ordre positionnel caractéristique des molécules présentes dans les colonnes n'est pas à longue portée⁵. En effet, la valeur quadratique moyenne des fluctuations positionnelles le long des colonnes varie linéairement en fonction de la taille du système mesurée perpendiculairement aux colonnes et la fonction de corrélation densité-densité le long des colonnes chute exponentiellement en fonction de la distance le long des colonnes. Toutefois, il a été montré plus récemment que l'hypothèse d'un couplage entre les degrés de liberté positionnels et orientationnels dans la phase D_{ho} des cristaux liquides en colonnes pourrait plutôt générer un quasi-ordre des molécules dans ces colonnes, avec une valeur quadratique moyenne pour les fluctuations positionnelles présen-

⁵P.-G. de Gennes et J. Prost, *The physics of liquid crystals*, 2nd Ed., Oxford University Press, New York, 1993.

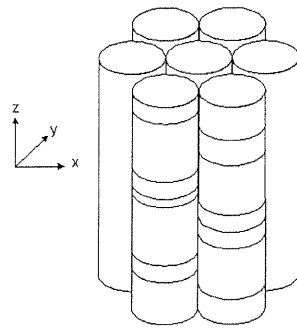


FIG. 6 – Structure hexagonale d'un cristal liquide en colonnes. Dans cette illustration, les distances intermoléculaires sont aléatoirement réparties le long de la direction des colonnes.

tant une divergence logarithmique en fonction de la taille du système mesurée perpendiculairement aux colonnes⁶. L'orientation des molécules dans ce cas est de type hélicoïdal : les molécules "tournent" à intervalles réguliers le long des colonnes, lesquelles possèdent des configurations d'hélicités bien déterminées. Une étude publiée récemment porte justement sur les diagrammes de phase des cristaux liquides en colonnes de type hexagonal⁷.

En conclusion, on ne peut donc pas qualifier pleinement la phase mésomorphe D_{ho} de phase ordonnée, mais tout au plus de phase quasi-ordonnée. Cependant, la question de savoir si cette phase s'apparente bel et bien à celle d'un cristal liquide ou à celle d'un vrai cristal demeure à ce jour non résolue.

⁶A. Caillé et M. Hébert, Phys. Rev. E **54**, R4544 (1996).

⁷G. Lamoureux, A. Caillé et D. Sénéchal, Phys. Rev. E **58**, 5898 (1998)

OBJECTIF DU TRAVAIL

Jusqu'à maintenant, aucune expérience n'a permis de conclure définitivement à la présence de quasi-ordre au sein d'un cristal liquide en colonnes dans la phase D_{ho} . En fait, aucun critère de vérification n'a été avancé qui permette, à partir d'expériences de diffraction par rayons X sur un tel cristal liquide, de confirmer ou d'infirmer l'hypothèse de la présence de quasi-ordre dans celui-ci. Le but de ce travail de maîtrise est donc d'établir un tel critère qui puisse par la suite servir de point de départ à des vérifications expérimentales. Plus précisément, nous voulons obtenir l'allure des décroissances en lois de puissance de l'intensité diffusée à proximité des maxima de Bragg qui résultent de la disposition des molécules le long des colonnes, de même que de la structure hélicoïdale incommensurable caractérisant leur orientation.

Pour ce faire, nous avons développé un modèle tri-dimensionnel simplifié mais réaliste de cristal liquide en colonnes dans la mésophase D_{ho} . Ce modèle, formé de la somme de deux densités de matière continues, est décrit dans la section II de l'article ci-joint. Par la suite, le calcul de l'effet des fluctuations thermiques de position et d'orientation des molécules sur l'intensité des rayons X diffusés (en assumant le couplage des degrés de liberté positionnels et orientationnels des molécules qui donne lieu au quasi-ordre au sein des colonnes) est décrit et réalisé en détail. Enfin, des expressions analytiques décrivant les décroissances en lois de puissance de ces intensités à proximité des maxima de Bragg sont obtenues.

Les résultats présentés dans ce mémoire permettent de rechercher expérimentalement la signature du quasi-ordre dans un cristal liquide en colonnes dans la mésophase D_{ho} . Nous suggérons donc que des mesures de l'intensité diffusée par des rayons X à haute intensité et haute résolution soient effectuées sur un échantillon d'un tel cristal liquide en colonnes afin de comparer celles-ci aux valeurs prédictes dans ce travail.

Thermal diffuse x-ray scattering in a model columnar liquid
crystal

Article soumis et accepté dans Physical Review E

Auteurs : A. Lacombe et A. Caillé

THERMAL DIFFUSE X-RAY SCATTERING IN A MODEL COLUMNAR LIQUID CRYSTAL

A. Lacombe and A. Caillé

*Département de physique, Université de Montréal, C.P. 6128, Succursale
Centre-Ville, Montréal, Québec, Canada H3C 3J7*

ABSTRACT

The fluctuation correlation functions and the density-density correlation functions for a realistic model of a columnar liquid crystal in its helically ordered phase are derived. The influence of positional and orientational molecular fluctuations on the thermal diffuse x-ray scattering is studied within a three-dimensional model of columns inscribed on a triangular lattice. Resulting from quasi-long-range orderings, very anisotropic long tail scattered intensities are predicted, giving a non-universal signature for the helically ordered columnar liquid crystal phase. Both scattered intensities near the Bragg maxima at the inverse lattice vectors and at the Bragg condition due to periodic orientational ordering are treated. The percolation of the long-range behaviour for a screw variable composed of two quantities having only quasi-long-range behaviour is predicted.

I. INTRODUCTION

Molecular systems in their condensed state show a great diversity of ordered phases involving their positional and orientational degrees of freedom. Partial positional and orientational orderings are present in mesomorphic systems such as the liquid crystals. Unique and new fundamental structural properties emerge from the complexity and richness of such ordered phases. One such manifestation is the existence of quasi-long-range positional order in

the layer ordering of smectic liquid crystals as revealed by the high-resolution thermal diffuse x-ray scattering measurements [1-3].

Among such molecular systems, a number of compounds composed of disk-shaped molecules show columnar liquid crystal phases, all sharing a two-dimensional lattice ordering of columns of stacked molecules in the third direction. The type of positional and orientational orderings existing, in these cases, along the columns and their intercolumnar correlations are issues of a fundamental nature. One-dimensional liquid-like columns are usually observed as predicted [4] by the divergent behaviour of the local fluctuations of the intracolumnar positional degrees of freedom for a two-dimensional lattice of freely sliding columns in the third direction. However, there do exist materials [5-7] where a full or partial ordering of these degrees of freedom sets in at lower temperatures with a simultaneous ordering of the orientational degrees of freedom along the columns.

These last cases reveal a fundamental issue of classification : do they belong to the crystal phases or the mesomorphous phases ? Up to now, this is still an open question [4,8-10]. However, the generally accepted understanding [5,6] calls for a long-range positional ordering inside the columns accompanied by an incommensurate helical orientational ordering of the discotic molecules along the columns. This model, which is derived from the observed Bragg peak positions and intensities [5,6], is at least inconsistent with the very large value (at least one third of the intermolecular spacing) of the phase-preserving vertical motion of the molecules [11] as measured from the Debye-Waller factors. Following these observations, in a previous publication [11], one of the authors has advanced the conjecture of quasi-long-range orderings of the positional and orientational degrees of freedom in such columnar liquid crystal. The vanishing of an effective shear elastic constant for strain deformations accompanied by a deformation of the orientational degrees of freedom would be at the origin of this behaviour in such soft material having an helically ordered state along the columns. As pre-

dicted [1] and observed [2,3] for smectic liquid crystals, thermal diffuse x-ray scattering in the presence of quasi-long-range ordering turns the Bragg peaks into Bragg maxima with a non-universal long tail decrease of the scattered intensity in reciprocal space. Such behaviour has been conjectured in [11] for a certain columnar liquid crystal by involving only the thermal fluctuations of the positional degrees of freedom along the columns.

In this paper, using a simplified but realistic model which captures the essential features of these systems, we calculate the effects of the thermal fluctuations of both the positional and orientational degrees of freedom along the columns on the thermal diffuse x-ray scattering. Our objective is to make specific predictions on the power law behaviour for the scattered intensity near the Bragg conditions resulting from both the ordering of the density of the molecules in the columnar direction and the incommensurate helical structure of their orientations. The three-column superlattice [5] existing for this frustrated intercolumnar structure is explicitly taken in account.

In section II, the model is presented explicitly with a description of the core density modulation in three dimensions. To this core density is added an orientational feature which captures the gross features of the incommensurate helical structure. Section III presents the local root mean square (rms) fluctuations of the positional and orientational degrees of freedom as a function of the size of the sample in a direction perpendicular to the direction of columns which are otherwise of infinite length. In section IV, the correlation functions for the density and orientational features are reported with their specific behaviour in two directions, namely parallel and perpendicular to the columns. Section V presents the calculations of thermal diffuse x-ray scattering intensities and their shapes in reciprocal space near the Bragg maxima. The calculations put the emphasis on the long tail behaviour of the intensity of the scattered x-rays for fluctuations controlled by quasi-long-range ordering. The classical behaviour, with a q^{-2} decrease, for fluctuating variables controlled by long-range ordering are assumed to exist and to be

buried under the non-classical behaviour due to quasi-long-range behaviour. Finally, the last section refers to specific interpretations and conclusions leading to further measurements of high intensity and high resolution diffuse x-ray scattering from these systems.

II. MODEL PRESENTATION

The molecular model for a liquid crystal made of disk-shaped molecules stacked into columns regularly placed onto a two-dimensional lattice, a structure known as a discotic, has already been investigated in details [5]. An example of such a liquid crystal is given by hexa-hexylthiotriphenylene (HHTT), one of the triphenylene derivatives whose molecules are formed of a rigid core of aromatic cycles and six flexible hydrocarbon chains fixed to the core. This compound shows two distinct hexagonal columnar phases : D_{hd} , a disordered columnar phase ($70^{\circ}\text{C} < T < 93^{\circ}\text{C}$) and H , a helically ordered columnar phase ($62^{\circ}\text{C} < T < 70^{\circ}\text{C}$). This last phase is of great interest since it could reveal, under given conditions, quasi-long-range intracolumnar order as proposed in [11]. In the H-phase phase, the lattice which supports the columns is reorganized in a superlattice $\sqrt{3} \times \sqrt{3}R30^{\circ}$ which is spanned by the set of vectors,

$$\vec{a}_1 = \frac{a}{2}(3\hat{x} + \sqrt{3}\hat{y}) \quad (1a)$$

$$\vec{a}_2 = a\sqrt{3}\hat{y} \quad (1b)$$

$$\vec{c}_1 = c\hat{z} \quad (1c)$$

where a is the distance between the centers of the columns in the basal plane and c is the distance between the molecules in the columns if long-range ordering is assumed as illustrated in Fig. 1(a) and 1(b). The superlattice conventional cell basis has three HHTT molecules located respectively at \vec{r}_j with $\vec{r}_0 = \vec{0}$, $\vec{r}_1 = \frac{1}{3}(\vec{a}_1 + \vec{a}_2) + \frac{1}{2}\vec{c}_1$ and $\vec{r}_2 = \frac{2}{3}(\vec{a}_1 + \vec{a}_2) + \frac{1}{2}\vec{c}_1$ as shown in Fig 1(a). The reciprocal lattice vectors associated with this lattice are given by

$\vec{K}_i(\vec{n}) = n_1 \vec{A}_1 + n_2 \vec{A}_2 + n_3 \vec{C}_1$ where n_1, n_2 and n_3 are integers and

$$\vec{A}_1 = \frac{4\pi}{3a} \hat{x} \quad (2a)$$

$$\vec{A}_2 = \frac{2\pi}{a} \left(\frac{1}{\sqrt{3}} \hat{y} - \frac{1}{3} \hat{x} \right) \quad (2b)$$

$$\vec{C}_1 = \frac{2\pi}{c} \hat{z}. \quad (2c)$$

For quasi-long-range order, this superlattice would only have a meaning in the \hat{z} -direction over a finite but extremely long distance measured on a molecular scale.

We choose to represent the density of molecules in the three-dimensional system by a development in a Fourier series which captures the essential features of the overall density modulation and which is called here the *core density*. The lower order components are sufficient for the study of the conversion of the lower order Bragg peaks into Bragg maxima and the calculations of the thermal diffuse scattering near those Bragg peaks. The coefficients of the Fourier series are chosen such that the core density (i) is real and positive everywhere, (ii) exhibits invariance with respect to a rotation of $\frac{2n\pi}{6}$ around the center of the zeroth column of every cell and (iii) is such that the maxima of the density for the columns numbered 1 and 2 are shifted by $\frac{c}{2}$ along the columnar axis with respect to the maxima of the columns numbered 0 [5]. Consequently, the equilibrium core density $\rho_{0c}(\vec{r})$, for an ordering extending to infinity, is written as :

$$\rho_{0c}(\vec{r}) = b_0 + \sum_{i \neq 0} b_{\vec{K}_i} \cos(\vec{K}_i \cdot \vec{r}) \quad (3)$$

where the specific relations between the real coefficients $b_{\vec{K}_i}$ are given below in order to satisfy the criteria mentioned above. For the purpose of calculating the density-density correlation functions appearing in the expression of the thermal diffuse scattering intensities near the lower order Bragg peaks, only a finite number of inverse lattice vectors have been selected, resulting in a

spatial density continuum instead of a discrete matter distribution. These vectors \vec{K}_i are

$$\begin{aligned} \vec{K}_i \in & \quad \{\vec{C}_1, \vec{A}_1 + \vec{C}_1, \vec{A}_1 - \vec{C}_1, \vec{A}_2 + \vec{C}_1, \vec{A}_2 - \vec{C}_1, -(\vec{A}_1 + \vec{A}_2) + \vec{C}_1, \\ & -(\vec{A}_1 + \vec{A}_2) - \vec{C}_1\} \cup \{2\vec{A}_1 + \vec{A}_2, -\vec{A}_1 + 2\vec{A}_2, \vec{A}_2 - \vec{A}_1\}. \end{aligned} \quad (4)$$

The first subset contains seven vectors describing the superlattice density and hence give no information about the inner-cell structure. Only the three vectors in the second subset of (4) generate an intra-cellular density modulation corresponding to the structure of the basis. The real coefficients $b_{\vec{K}_i}$ associated with the different \vec{K}_i 's must verify the following relations :

$$b_0 = \sum_{i=1}^{10} b_{\vec{K}_i}, \quad (5a)$$

$$b_{\vec{K}_2} = b_{\vec{K}_3} = b_{\vec{K}_4} = b_{\vec{K}_5} = b_{\vec{K}_6} = b_{\vec{K}_7}, \quad (5b)$$

$$b_{\vec{K}_8} = b_{\vec{K}_9} = b_{\vec{K}_{10}}, \quad (5c)$$

and

$$b_{\vec{K}_1} = -\frac{1}{4} \left(\sum_{i=2}^7 b_{\vec{K}_i} \right), \quad (5d)$$

where the vectors \vec{K}_i are numbered in the order they appear in (4) : $\vec{K}_1 = \vec{C}_1$, $\vec{K}_2 = \vec{A}_1 + \vec{C}_1$, $\vec{K}_3 = \vec{A}_1 - \vec{C}_1$, and so on (note that $\vec{K}_0 = \vec{0}$). The condition (5a) ensures that ρ_{0c} is positive everywhere ; (5b) and (5c) result from the rotational invariance constraint (ii) described above while (5d) follows from the constraint (iii). The equilibrium core density continuum is illustrated in Fig. 2. The superlattice structure in the basal plane is easily seen as well as the displacement in the columnar direction of two-third of the columns.

The second feature to capture in the density is the helical modulation appearing as we move along the columnar direction. For the purpose of representing this density modulation, a term is added to (3). This term accounts for the geometry and orientation of HHTT molecules. Effectively, these disk-like molecules in their propeller configuration [6] show a rotational invariance of $\frac{2n\pi}{3}$ around an axis passing through their center, perpendicularly to their

planar central core. Thus, around every site along the column j , a supplementary density modulation proportional to $\cos 3(\theta - \theta_{0j}(z))$ is added on a circle of radius R_0 placed perpendicularly to the columnar direction and centered on the site as depicted in Fig. 3. R_0 is the mean radius of the molecular columns which are extending in the z-direction. The phase $\theta_{0j}(z)$, representing the angular shift of the molecules along the column j in the equilibrium helical conformation, is written as :

$$\theta_{0j}(z) = H_j \omega z + \Omega_j \quad (6)$$

where H_j and Ω_j are respectively the helicity ($H_j = \pm 1$) and the rigid angular shift of the column j . ω equals $\frac{2\pi}{P}$ where P is the pitch of the column. In the present model, P will be taken close to $8c$, every molecule being rotated by an amount close to $\frac{\pi}{4}$ from its nearest neighboring molecule inside a given column. Incommensurability between the pitch and the lattice distance has been assumed for the present work even though this is still an open question [13]. Also, the rotational invariance constraint (ii) implies that $H_1 = H_2$ and $\Omega_1 = \Omega_2$. In the present model, this helicoïdal density engraving is called the *groove density* and is written as

$$\rho_{g0}(\vec{r}) = \rho_0 \sum_{n,m} \sum_{j=0}^2 \delta(\vec{\rho} - (\vec{\rho}_{nm} + \vec{\rho}_j + \vec{\sigma})) \cos 3(\theta - H_j \omega z - \Omega_j) \quad (7)$$

where cylindrical coordinates have been used. $\vec{r} = (\vec{\rho}, z)$ with $\vec{\rho} = (\rho, \alpha_\perp)$, as illustrated in Fig. 4. The discrete molecular density modulation has been represented, for simplicity, by a continuous cylindrical surface density modulation. These density modulation cylinders of radius R_0 are centered on the lattice points given by $\vec{\rho}_{nm} + \vec{\rho}_j$ where $\vec{\rho}_{nm} = n\vec{a}_1 + m\vec{a}_2$ and $\vec{\rho}_j = \frac{j}{3}(\vec{a}_1 + \vec{a}_2)$ with $j \in \{0, 1, 2\}$. Finally, $\vec{\sigma}$ ($\vec{\sigma} = (R_0, \theta)$) points at a specific location on the surface density modulation cylinder (see Fig. 4). The constant coefficient ρ_0 in (7) is chosen to ensure that the total density remains positive everywhere. Thus, the total equilibrium density, according to the model developed here for the HHTT discotic liquid crystal in its H phase, is given by

$\rho_0(\vec{r}) = \rho_{c0}(\vec{r}) + \rho_{g0}(\vec{r})$. Although this separation of the density modulation into two terms is not derived from first principles, it has the advantage to capture the essential features affecting the diffuse x-ray scattering near the lower order Bragg peaks.

III. LOCAL CORRELATION FUNCTIONS

In this section, the local root mean square (rms) fluctuations of the positional and orientational degrees of freedom of the molecules are presented. In the next section, these results are used to establish the behaviour of the density-density correlation function $\langle \rho(\vec{r})\rho(\vec{r}') \rangle$ along specific directions in our columnar liquid crystal model. The details of the calculations are presented in the appendix.

Among all the possible positional fluctuations of the molecules, only the displacement $u_z(\vec{r})$ along the columnar direction have been considered. This limitation will be justified later in section VI. The orientational fluctuations of the molecules are described by $\varphi(\vec{r})$, an angular variable specifying a rotation in the plane perpendicular to the columns with respect to the helical equilibrium conformation. The planar positional fluctuations $u_{q\perp}(\vec{r})$ have not been considered in the density fluctuations since they are known to have long-range behaviour in this phase [4]. The fluctuating density is written as $\rho(\vec{r}) = \rho_0(\vec{r} - u_z(\vec{r})\hat{z})$ where ρ_0 represents the density of the system at $T = 0^\circ\text{K}$ [12]. Taking $\rho_{c0}(\vec{r}) + \rho_{g0}(\vec{r})$ as the equilibrium density ρ_0 , the fluctuations are introduced both in $\rho_{c0}(\vec{r})$ and $\rho_{g0}(\vec{r})$ according to :

$$\rho_c(\vec{r}) = b_0 + \sum_{i \neq 0} b_{\vec{K}_i} \cos(K_{i\perp}\rho \cos(\alpha_\perp - \alpha_i) + K_{iz}(z - u_z(\vec{r}))) \quad (8)$$

for the fluctuating core density and to :

$$\begin{aligned} \rho_g(\vec{r}) = & \rho_{g0} \sum_{n,m} \sum_{j=0}^2 \delta(\vec{\rho} - (\vec{\rho}_{nm} + \vec{\rho}_j + \vec{\sigma})) \\ & \times \cos 3(\theta - H_j \omega(z - u_z(\vec{r})) - (\Omega_j - \varphi(\vec{r}))) \end{aligned} \quad (9)$$

for the fluctuating groove density. α_i is the angle between \vec{K}_i and \hat{x} .

A derivation of the total elastic energy, based on the orientational and positional elastic energy densities, has been carried out by one of the authors in [11]. The diagonalized form of this total elastic energy, expressed in Fourier space using cylindrical coordinates, is given by

$$E = \frac{1}{2(2\pi)^3} \int d^3q \left\{ \left[g_1 - \frac{\gamma^2}{4g_2} \right] |u_z(\vec{q})|^2 + g_2 |u'_{q\perp}(\vec{q})|^2 + \left[\frac{1}{4} C_5 q_z^2 + C_3 q_\perp^2 \right] |u_\theta(\vec{q})|^2 + f |\Psi(\vec{q})|^2 \right\} \quad (10)$$

where the functions $g_1(\vec{q})$, $g_2(\vec{q})$, $\gamma(\vec{q})$, $f(\vec{q})$, $a(\vec{q})$ and $b(\vec{q})$ are defined in [11]. The quantities A_i , B_i , C_i , and K_i appearing here or into the following equations are the elastic constants introduced in [11]. In the process of diagonalization, two successive changes of variables are introduced, leading to :

$$\varphi(\vec{q}) = \Psi(\vec{q}) - \frac{b}{2f} u_z(\vec{q}) - \frac{a}{2f} u_{q\perp}(\vec{q}) \quad (11)$$

and

$$u_{q\perp}(\vec{q}) = u'_{q\perp}(\vec{q}) - \frac{\gamma}{2g_2} u_z(\vec{q}). \quad (12)$$

From (10), the theorem of equipartition yields

$$\langle |u_z(\vec{q})|^2 \rangle_T = \frac{k_B T}{g_1 - \frac{\gamma^2}{4g_2}}, \quad (13a)$$

$$\langle |u'_{q\perp}(\vec{q})|^2 \rangle_T = \frac{k_B T}{g_2}, \quad (13b)$$

$$\langle |u_\theta(\vec{q})|^2 \rangle_T = \frac{k_B T}{\frac{1}{4} C_5 q_z^2 + C_3 q_\perp^2}, \quad (13c)$$

and

$$\langle |\Psi(\vec{q})|^2 \rangle_T = \frac{k_B T}{f} \quad (13d)$$

for the rms fluctuations expressed in Fourier space. The brackets with the subscript T denote an average over all the thermal states.

In the long wavelength limit, the denominator of (13a) has the following power expansion for $q_\perp \ll q_z$:

$$g_1 - \frac{\gamma^2}{4g_2} = C_1 q_z^2 + G q_\perp^2 \quad (14)$$

where $G = C_5/4 - (C_4 + \frac{1}{2}C_5)^2/2C_5$. (14) is typical of a denominator for long-range ordering where the local rms fluctuation of the vertical displacement would have a microscopic value proportional to a molecular length, a value independent of the size of the system.

For $q_z \ll q_\perp$, the long wavelength limit expression for the denominator becomes

$$g_1 - \frac{\gamma^2}{4g_2} = C_1 q_z^2 + K q_\perp^4 \quad (15)$$

where $K = B_2^2(K_1 + K_2)/8A_1^2$, provided that the hypothesis of an effective free sliding of ordered columns on each other is realized [11].

The thermal and space average $\langle u_z^2(\vec{r}) \rangle$ is given by :

$$\langle u_z^2(\vec{r}) \rangle = \frac{1}{V} \frac{1}{(2\pi)^3} \int d^3 q \langle |u_z(\vec{q})|^2 \rangle_T \quad (16)$$

where V is the volume of the system. The integral in (16) is dominated by a size dependent term arising from the integrand in the long wavelength limit and $q_z \ll q_\perp$. The rest of the integral adds only size independent terms of microscopic magnitude. The size dependent term is easily shown to be given by :

$$\langle u_z^2(\vec{r}) \rangle = \frac{k_B T}{4\pi \sqrt{KC_1}} \ln \left(\frac{L_\perp}{a} \right), \quad (17)$$

an expression involving only the size L_\perp of the system in a direction perpendicular to the columns with otherwise infinite length. This expression which increases progressively but slowly with the length L_\perp is typical of quasi-long-range order [11].

The calculation of $\langle u_z(\vec{r})\varphi(\vec{r}) \rangle$ is carried out in section 1 of the appendix using the residue theorem in the complex plane and yields :

$$\langle u_z(\vec{r})\varphi(\vec{r}) \rangle = \frac{-k_B T}{4\pi \sqrt{KC_1}} \frac{B_2}{8A_1} \ln \left(\frac{L_\perp}{a} \right). \quad (18)$$

under the same approximations as above. Again, this result involves only the size of the sample in the direction perpendicular to the columns.

The third local rms fluctuation correlation function, $\langle \varphi^2(\vec{r}) \rangle$, involves three separate integrations over the Fourier space since the diagonalized form of $\varphi(\vec{r})$ is the sum of three independent fluctuating quantities according to (11) and (12). The final result is given by

$$\begin{aligned} \langle \varphi^2(\vec{r}) \rangle = & \frac{k_B T}{4\pi\sqrt{(K_1 + K_2)A_2}} \ln(K' + \sqrt{K'^2 + 1}) + \frac{k_B T}{4\pi\sqrt{KC_1}} \frac{B_2^2}{16A_1^2} \ln\left(\frac{L_\perp}{a}\right) \\ & + C' \frac{k_B T}{a} \frac{(B_1 + B_2)^2}{A_2^2 C_5} \end{aligned} \quad (19)$$

where K' and C' are constants defined in section 1 of the appendix. A striking feature of the first and third terms of (19) is that they are independent of the size of the sample. These terms arise respectively from the integration of $\langle |\Psi(\vec{q})|^2 \rangle_T$ and $\frac{a^2}{4f^2} \langle |u'_{q_\perp}(\vec{q})|^2 \rangle_T$ over the Fourier space, indicating that these quantities have behaviours typical of long-range orderings.

IV. FLUCTUATION CORRELATION FUNCTIONS AND DENSITY-DENSITY CORRELATION FUNCTIONS

The density-density correlation functions involve not only the local fluctuation correlation functions but also the fluctuation correlation functions. $\langle u_z(\vec{r})u_z(\vec{r}') \rangle$, $\langle u_z(\vec{r})\varphi(\vec{r}') \rangle$, $\langle u_z(\vec{r}')\varphi(\vec{r}) \rangle$ and $\langle \varphi(\vec{r})\varphi(\vec{r}') \rangle$ are obtained in the next subsection. The density-density correlation functions are then calculated using these results and those of section III.

A. Fluctuation correlation functions in the columnar direction

In this subsection, only the results are presented, the reader being referred to section 2 of the appendix for further mathematical details. The first correlation function of interest is $\langle u_z(\vec{r})u_z(\vec{r}') \rangle$. Assuming overall translational

invariance, it is given by :

$$\langle u_z(\vec{r})u_z(\vec{r}') \rangle = \int \frac{d^3q}{(2\pi)^3} \langle |u_z(\vec{q})|^2 \rangle_T e^{-i\vec{q}\cdot(\vec{r}-\vec{r}')} . \quad (20)$$

Let us start with the correlation for large separation along the columns, ie $|z - z'| \gg c$ and $|\rho - \rho'|$ of the order of a . As a result, the integral (20) is dominated by the small q_z contributions where q_\perp extends from its lower limit $2\pi/L_\perp$ to $2\pi/a$. Consequently, $\langle |u_z(\vec{q})|^2 \rangle$ is governed by the denominator (15). As shown in the appendix, $\langle u_z(\vec{r})u_z(\vec{r}') \rangle$ is then given by :

$$\langle u_z(\vec{r})u_z(\vec{r}') \rangle = \frac{-k_B T}{8\pi\sqrt{KC_1}} \left[2\gamma + E_1\left(\frac{(\rho - \rho')^2}{4\beta|z - z'|}\right) + \ln\left(\frac{\pi^2(\rho - \rho')^2}{L_\perp^2}\right) \right] \quad (21)$$

It has been assumed in the calculation of (21) that $\vec{\rho}$ is parallel to $\vec{\rho}'$ since only quantities dependent on $\vec{\rho} - \vec{\rho}'$ will be needed in the subsequent calculations. The fluctuation correlation function $\langle u_z(\vec{r})\varphi(\vec{r}') \rangle$, under similar conditions, is given by :

$$\begin{aligned} \langle u_z(\vec{r})\varphi(\vec{r}') \rangle = & \frac{k_B T}{8\pi\sqrt{KC_1}} \frac{B_2}{4A_1} \left[2\gamma + E_1\left(\frac{(\rho - \rho')^2}{4\beta|z - z'|}\right) \right. \\ & \left. + \ln\left(\frac{\pi^2(\rho - \rho')^2}{L_\perp^2}\right) \right]. \end{aligned} \quad (22)$$

The fluctuation correlation function $\langle \varphi(\vec{r})\varphi(\vec{r}') \rangle$ involves three separate integrations, as in (A9). Assuming again that $\vec{\rho}$ is parallel to $\vec{\rho}'$, this quantity, under the same conditions as above, is given by :

$$\begin{aligned} \langle \varphi(\vec{r})\varphi(\vec{r}') \rangle = & \frac{k_B T}{8\pi} \sum_{i=1}^4 \frac{\xi_i}{\sqrt{\kappa_i(z - z')^2 + (\rho - \rho')^2}} \\ & - \frac{k_B T}{8\pi\sqrt{KC_1}} \frac{B_2^2}{16A_1^2} \left[2\gamma + E_1\left(\frac{(\rho - \rho')^2}{4\beta|z - z'|}\right) \right. \\ & \left. + \ln\left(\frac{\pi^2(\rho - \rho')^2}{L_\perp^2}\right) \right] \end{aligned} \quad (23)$$

where the constant coefficients ξ_i and κ_i are defined in the appendix.

B. Fluctuation correlation functions in the direction perpendicular to the columns

As shown in section 3 of the appendix, the fluctuation correlation functions at large separation in the plane perpendicular to the columns for a separation along the columns of a molecular size ($|z - z'| \sim c$ and $|\rho - \rho'| \gg a$) follow a behaviour typical of long-range ordering. Effectively, under these conditions, the integral (20) is dominated by the small q_\perp contributions where q_z extends from $-\infty$ to ∞ , the denominator in action being given by (14).

C. Density-density correlation functions in the columnar direction

In this subsection, the behaviour of the density-density correlation function $G(\vec{r} - \vec{r}') = \langle \rho(\vec{r})\rho(\vec{r}') \rangle$ is presented for the columnar direction. According to the present model, this function is given by :

$$\begin{aligned} G(\vec{r} - \vec{r}') &= \langle \rho(\vec{r})\rho(\vec{r}') \rangle \\ &= \langle [\rho_c(\vec{r}) + \rho_g(\vec{r})][\rho_c(\vec{r}') + \rho_g(\vec{r}')] \rangle \\ &= \langle \rho_c(\vec{r})\rho_c(\vec{r}') \rangle + \langle \rho_c(\vec{r})\rho_g(\vec{r}') \rangle \\ &\quad + \langle \rho_g(\vec{r})\rho_c(\vec{r}') \rangle + \langle \rho_g(\vec{r})\rho_g(\vec{r}') \rangle \end{aligned} \quad (24)$$

where the brackets denote spatial and thermal averages, and $\rho(\vec{r})$ and $\rho(\vec{r}')$ are given by (8) and (9). These calculations are performed by using the fact that for fluctuating quantities x_i subject to a Gaussian distribution, the relation

$$\langle \exp[\alpha_i x_i] \rangle_T = \exp[\alpha_i \alpha_k \langle x_i x_k \rangle_T / 2] \quad (25)$$

where the α_i are constants, always holds [12]. It is found, as detailed in section 4 of the appendix, that only the terms $\langle \rho_c(\vec{r})\rho_c(\vec{r}') \rangle$ and $\langle \rho_g(\vec{r})\rho_g(\vec{r}') \rangle$ contribute to $G(\vec{r} - \vec{r}')$. Effectively, the mixed terms $\langle \rho_c(\vec{r})\rho_g(\vec{r}') \rangle$ and $\langle \rho_g(\vec{r})\rho_c(\vec{r}') \rangle$ vanish in the averaging process over thermal states unless $K_{iz} = \pm 3(H_j \omega \pm \frac{B_2}{4A_1})$, or $K_{iz} = \pm 3(H_{j'} \omega \pm \frac{B_2}{4A_1})$, conditions which are too restrictive.

The behaviour of the first term of $G(\vec{r} - \vec{r}')$ along the columnar direction (for $|z - z'| \gg c$ and $|\rho - \rho'| \simeq a$) is given by

$$\langle \rho_c(\vec{r}) \rho_c(\vec{r}') \rangle \sim \sum_i b_{K_i}^2 \cos \vec{K}_i \cdot (\vec{r} - \vec{r}') \left(\frac{a^2}{4\pi^2 \beta |z - z'|} \right)^{X(K_{iz})}, \quad (26)$$

with

$$X(K_{iz}) = K_{iz}^2 \frac{k_b T}{8\pi \sqrt{KC_1}}. \quad (27)$$

The behaviour of the last term is given by

$$\langle \rho_g(\vec{r}) \rho_g(\vec{r}') \rangle \sim \sum_{n,m} \sum_{n',m'} \sum_{j=0}^2 \sum_{j'=0}^2 F_2 \left(\frac{a^2}{4\pi^2 \beta |z - z'|} \right)^{X'_j} \quad (28)$$

within the same limit as in (26), with

$$F_2 = \delta(\vec{\rho} - (\vec{\rho}_{nm} + \vec{\rho}_j + \vec{\sigma})) \delta(\vec{\rho}' - (\vec{\rho}_{n'm'} + \vec{\rho}_{j'} + \vec{\sigma}')) \times \cos 3(\theta - H_j \omega z - \Omega_j - (\theta' - H_{j'} \omega z' - \Omega_{j'})). \quad (29)$$

and

$$X'_j = \frac{9k_b T}{8\pi \sqrt{KC_1}} \left(\frac{B_2}{4A_1} - H_j \omega \right)^2. \quad (30)$$

This last exponent involves explicitly the value of the helicity of the j th column.

D. Density-density correlation function in a direction perpendicular to the columns

In parallel with the results reported in subsection B, the density-density correlation functions at large separation in the plane perpendicular to the columns ($|z - z'| \sim c$ and $|\rho - \rho'| \gg a$) are, under the above conditions, typical of long-range ordering. As a result, they are periodic functions with the periods of the columns in the two-dimensional basal plane.

V. X-RAY SCATTERED INTENSITIES

In this section, the scattered intensities for both the non-fluctuating and the fluctuating equilibrium conformations of our model are presented. The general expressions found for the density-density correlation functions derived above are used.

A. The Bragg conditions of the model

The x-ray scattering intensity for a momentum transfer \vec{Q} is obtained directly from the Fourier transforms of $\rho_c(\vec{r})$ according to :

$$I(\vec{Q}) \propto \int d^3r \int d^3r' \rho(\vec{r})\rho(\vec{r}') e^{i\vec{Q} \cdot (\vec{r} - \vec{r}')} \quad (31)$$

where proportionality constants are omitted. The scattering intensity is decomposed into three terms according to :

$$I(\vec{Q}) = I_{cc}(\vec{Q}) + I_{cg}(\vec{Q}) + I_{gg}(\vec{Q}). \quad (32)$$

The indices refer to the different combinaisons of core density and groove density in the decomposition of the total density $\rho(\vec{r})$. It is easily shown that the mixed term I_{cg} does not contribute and that I_{cc} is the only term contributing to the scattering near the inverse lattice vectors and conversely only the term I_{gg} contributes for scattering near the Bragg condition due to the periodic orientational density. In the absence of thermal fluctuations, the result is :

$$\begin{aligned} I(\vec{Q}) &\propto \sum_i b_{\vec{K}_i}^2 \delta_{\vec{Q}, \pm \vec{K}_i} + \rho_{g0}^2 J_3^2(Q_\perp R_0) \\ &\times \left(1 + 4 \sin^2 \left(\frac{2}{3} \vec{Q}_\perp \cdot (\vec{a}_1 + \vec{a}_2) \right) \right) \delta_{Q_z, \pm 3\omega} \delta_{\vec{Q}_\perp, \vec{K}_{hk}} \end{aligned} \quad (33)$$

where $\vec{K}_{hk} = p\vec{A}_1 + k\vec{A}_2$ and J_3 is the third order Bessel function. The first term in (33) is proportional to the Fourier transform of $\rho_c(\vec{r})\rho_c(\vec{r}')$, while

the second term is proportional to the Fourier transform of $\rho_g(\vec{r})\rho_g(\vec{r}')$. The scalar product in this latter term could be rewritten as :

$$\frac{2}{3}\vec{Q}_\perp \cdot (\vec{a}_1 + \vec{a}_2) = \frac{4\pi}{3}(p+k) \quad (34)$$

since $\vec{Q}_\perp = p\vec{A}_1 + k\vec{A}_2$.

B. The thermal diffuse x-ray scattering near the reciprocal lattice vectors

The scattered intensity of x-rays for a momentum transfer \vec{Q} when the thermal fluctuations are included is given by :

$$I(\vec{Q}) = \int d^3r \int d^3r' \langle \rho(\vec{r})\rho(\vec{r}') \rangle e^{i\vec{Q} \cdot (\vec{r}-\vec{r}')} \quad (35)$$

where $\langle \rho(\vec{r})\rho(\vec{r}') \rangle$ is the density-density correlation function averaged over the thermal fluctuations. We now consider a momentum transfer \vec{Q} close to the reciprocal lattice vectors \vec{K}_i such that $\vec{Q} = \vec{K}_i + \vec{q}_\perp + q_z \hat{z}$ where \vec{q}_\perp and q_z are very small on the scale of the inverse of their respective intermolecular distances.

Within our model, the scattering intensity near the reciprocal lattice vectors are limited to the basal plane $K_{iz} = 0$ and the planes $\vec{K}_{iz} = \pm \vec{C}_1$. The shapes of the Bragg peaks in the basal plane $K_{iz} = 0$ are easily predicted. Indeed only the thermal fluctuations of the perpendicular component \vec{u}_\perp determine the diffuse scattering of the x-rays for a zero value of K_{iz} . Since this quantity reflects the long-range ordering in the basal plane, the Bragg peaks in this plane maintain their character with an intensity controlled by a Debye-Waller factor and a decrease in reciprocal space which is inversely proportional to the square of the wavenumber departure from the Bragg positions.

For the planes at $\vec{K}_{iz} = \pm \vec{C}_1$, the thermal fluctuations of u_z turn the Bragg peaks into Bragg maxima with a non universal behaviour of the power

law decrease of the scattered intensity in reciprocal space. Near the Bragg conditions for the lattice, the scattered intensity is written as :

$$I_{cc}(q_z, \vec{q}_\perp) \propto \int d^3r e^{iq_z z} e^{i\vec{q}_\perp \cdot \vec{r}} \left[e^{i\vec{K}_i \cdot \vec{r}} \langle \rho_c(\vec{r}) \rho_c(0) \rangle \right]. \quad (36)$$

For $q_z \simeq 0$ and $q_\perp \gg q_z$, the integral (36) is dominated by a cone surrounding the z-axis and extending to infinity. The correlation function of the fluctuating displacements in this cone is then given by expression (21). As a result, $I_{cc}(q_z, \vec{q}_\perp)$ is easily shown to become :

$$\begin{aligned} I_{cc}(\vec{Q}) \propto & b_{\vec{K}_i}^2 \int_{-\infty}^{\infty} dz \int_0^{\infty} \rho d\rho J_0(q_\perp \rho) \\ & \times \exp \left[iq_z z - X(K_i) \left(2\gamma + E_1 \left(\frac{\rho^2}{4\beta|z|} \right) \right) \right] \left(\frac{a}{\pi\rho} \right)^{2X(K_i)} \end{aligned} \quad (37)$$

where a first integration over the angular part in the basal xy plane has been performed. The changes of variables $w = \rho^2/4\beta|z|$ and $z' = q_z z$ yields :

$$\begin{aligned} I_{cc}(\vec{Q}) \propto & \sum_i b_{\vec{K}_i}^2 \frac{1}{q_z^{2-X(K_i)}} \int_0^{\infty} dz' z'^{1-X(K_i)} \exp(iz') \\ & \times \int_0^{\infty} dw w^{-X(K_i)} \exp[-X(K_i)E_1(w)] J_0 \left(2q_\perp \sqrt{\frac{\beta z' w}{q_z}} \right). \end{aligned} \quad (38)$$

Using scaling techniques, the two integrals in (38) can easily be shown to be proportional to $(q_z/q_\perp^2)^{2-X(K_i)}$, thus yielding :

$$I_{cc}(\vec{Q}) \propto \sum_i b_{\vec{K}_i}^2 \frac{1}{q_\perp^{4-2X(K_i)}} , \text{ for } q_z = 0. \quad (39)$$

The calculation of $I_{cc}(\vec{Q})$ when $q_\perp \simeq 0$ and $q_z \gg q_\perp$ is not explicitly given. The scattering intensity is typical of a crystalline structure [4]. Indeed, under this condition, the system exhibits long-range order behaviour, as discussed in the third section of the appendix. The result is :

$$I_{cc}(\vec{Q}) \sim \frac{1}{q_z^2} , \text{ for } q_\perp = 0. \quad (40)$$

C. Thermal diffuse scattering near the Bragg condition due to the periodic orientation density

The thermal diffuse scattering of x-rays under those conditions is calculated from $I_{gg}(\vec{Q})$, with a momentum transfer $\vec{Q} = \vec{K}_{hk} + \vec{q}_\perp + 3\omega\hat{z} + q_z\hat{z}$ where \vec{q}_\perp and q_z are very small on the scale of the inverse of their respective intermolecular dimension.

It is found that the thermal fluctuations of φ and u_z turn the Bragg peaks at $Q_z = \pm 3\omega$ into Bragg maxima with a universal behaviour of the power law decrease of the scattered intensity in reciprocal space. Effectively, near these Bragg conditions, the scattered intensity is written as :

$$I_{gg}(q_z, \vec{q}_\perp) \propto \int d^3r e^{iq_z z} e^{i\vec{q}_\perp \cdot \vec{r}} \int d^3r' e^{-i\vec{Q} \cdot \vec{r}'} \left[e^{i\vec{K}_{hk} \cdot \vec{r}'} e^{i3\omega z} \langle \rho_g(\vec{r}) \rho_g(\vec{r}') \rangle \right]. \quad (41)$$

where $\vec{r}' = \vec{r}_{j'} + \vec{\sigma}'$ (ie $\vec{r}_{n'm'} = \vec{0}$ and $z' = 0$).

As discussed in the previous subsection, for $q_z \simeq 0$ and $q_\perp \gg q_z$, the integral (41) is dominated by a cone surrounding the z-axis and extending to infinity. The correlation functions of the fluctuating quantities are then given by (21) and (23). As shown in the section 5 of the appendix, $I_{gg}(q_z, \vec{q}_\perp)$ becomes

$$\begin{aligned} I_{gg}(\vec{Q}) \propto & \frac{J_3^2(K_{hk}R_0)}{q_z^{2-X'_0}} \int_0^\infty dz' \exp[iz'] z'^{1-X'_0} \int_0^\infty dw w^{-X'_0} \exp[-X'_0 E_1(w)] \\ & \times J_0\left(2q_\perp \sqrt{\frac{w\beta z'}{3q_z}}\right) \prod_{i=1}^4 \exp[-\xi_i(\tau_i z'^2 + \tau' \omega |z'|)^{-1/2}] \\ & + \frac{2J_3^2(K_{hk}R_0)(1 + \cos(\vec{q}_\perp \cdot (\vec{r}_2 - \vec{r}_1)))}{q_z^{2-X'_1}} \int_0^\infty dz' \exp[iz'] z'^{1-X'_1} \\ & \times \int_0^\infty dw w^{-X'_1} \exp[-X'_1 E_1(w)] \\ & \times J_0\left(2q_\perp \sqrt{\frac{w\beta z'}{3q_z}}\right) \prod_{i=1}^4 \exp[-\xi_i(\tau_i z'^2 + \tau' \omega |z'|)^{-1/2}] \end{aligned} \quad (42)$$

where $\tau_i = \kappa_i/9q_z^2$ and $\tau' = 4\beta/3|q_z|$. Using scaling techniques, the two integrals in the first term of (42) are found to be proportional to $q_z^{2-X'_0}/\sqrt{q_\perp}$,

while the two integrals in the second term of (42) are found to be proportional to $q_z^{2-X_1'}/\sqrt{q_\perp}$, leading to :

$$I_{gg}(\vec{Q}) \propto \frac{J_3^2(K_{hk}R_0)}{\sqrt{q_\perp}} (3 + 2 \cos(\vec{q}_\perp \cdot (\vec{\rho}_2 - \vec{\rho}_1))) , \text{ for } q_z = 0. \quad (43)$$

As for I_{cc} , the calculation of $I_{gg}(\vec{Q})$ when $q_\perp \simeq 0$ with $q_z \gg q_\perp$ is not explicitly given. The scattering intensity is typical of a crystalline structure [4]. The result is :

$$I_{gg}(\vec{Q}) \sim \frac{1}{q_z^2} , \text{ for } q_\perp = 0. \quad (44)$$

VI. DISCUSSION AND CONCLUSION

It is important to recall that our calculations are based on a model admitting the orderings of the positional and orientational degrees of freedom of the discotic molecules along the columns, as is generally admitted [5,6,11]. In particular, it is based on the existence of an incommensurate helically ordered density wave along the columnar direction. This density wave results from the ordering of the orientational degrees of freedom. Our model differs from those in the literature only on the range of the ordering, quasi-long-range being speculated in our case.

The separation of the total density $\rho(\vec{r})$ into a core density term $\rho_c(\vec{r})$ and a groove density term $\rho_g(\vec{r})$ is not derived from first principles. In addition, it is clear also that these two quantities are coupled since a core density fluctuation along the columns would break locally the periodic orientational modulation. However, these two quantities refer to independent degrees of freedom to first order : the displacements of the centers of mass of the molecules in the columnar direction and the orientation of the molecules in a plane perpendicular to this direction. This separation captures the two essential features of the density, exactly these features which separately, to lowest order, determine the Bragg conditions for the inverse lattice vectors and the periodic orientational density. Our work is not intended to calculate

the intensities of the Bragg maxima but to predict the power law behaviour followed by the thermal diffuse x-ray scattering intensities near the Bragg conditions. For such a calculation, we argue that the above separation is justified.

The origin of all the results presented above is the behaviour of the denominator of (13a) governing the rms fluctuations $\langle |u_z(\vec{q})|^2 \rangle_T$. The quadratic form in (14) reflects the fact that a fluctuation $u_z(\vec{q})$ with a wavelength in the plane perpendicular to the columns very large compared to the length scale of the modulation along the columns, in other words neighboring columns moving in phase in the columnar direction, is unaffected by the free sliding of the rotating neighboring columns. However, the free sliding of the rotating columns on each other is reflected in the q_\perp^4 behaviour for a fluctuation $u_z(\vec{q})$ with a wavelength in the plane perpendicular to the columns very small compared to the length scale of the modulation along the columns. It is this last property which gives rise to the quasi-long-range behaviour. Indeed, $\langle u_z^2(\vec{r}) \rangle$ shows a quasi-long-range behaviour as reflected in (17). On the contrary, $\langle u_{q\perp}^2(\vec{r}) \rangle$ shows a long-range behaviour as reported in (19). This last behaviour justifies that $\langle u_{q\perp}^2 \rangle_T$ is neglected in the calculation of the long tail behaviour of the scattered intensities.

The negative sign of the local fluctuation function $\langle u_z(\vec{r})\varphi(\vec{r}) \rangle$ points to the fact that the independent fluctuating quantity $\Psi(\vec{q})$ is the sum of a rotation $\varphi(\vec{q})$ and a displacement $u_z(\vec{q})$ in the columnar direction, operating in opposite direction in the long wavelength limit for $q_z \ll q_\perp$, in other words when neighboring columns are moving more or less rigidly in the columnar direction. Notice that the composite rotation angle $\Psi(\vec{r})$ shows a long-range behaviour percolating through the quasi-long-range behaviours of $u_z(\vec{r})$ and $\varphi(\vec{r})$.

The fluctuation correlation functions show a very anisotropic behaviour. Indeed, these quantities in the columnar direction have only a quasi-long-range behaviour while in the direction perpendicular to the columnar direc-

tion, a long-range ordering behaviour is predicted. As indicated above, these reflect the wave number dependence of $\langle u_z^2(\vec{r}) \rangle$. As a result, the core density-core density correlation function in the columnar direction shows power law behaviour with a series of exponents determined by the elastic constants. The groove density-groove density correlation function in the columnar direction shows a similar power law behaviour with exponents related to the helicities of the columns. The correlation functions in the basal plane show long-range behaviour.

As mentioned above, our simplified model is not suitable for calculating the relative intensities of the different Bragg peaks. However, it is reasonably justified to calculate the effect of thermal fluctuations on the shape of the Bragg maxima. The first result of interest is that the Bragg peaks in the basal plane $K_{iz} = 0$ retain a behaviour typical of long-range ordering. We have not explicitly calculated the effect of the thermal diffuse x-ray scattering and the shape of the intensity contours in this case. This calculation is straightforward and would involve taking in account the effects of the fluctuations $u_{q\perp}(\vec{q})$. The results would be classical and should show anisotropic intensity contours resulting from the anisotropy of the elastic constants. Such behaviour has been studied [14] for the freely suspended strands of a discotic liquid crystal in the intracolumnar disordered phase. It is to be noted that in this last case, the Bragg peaks are limited to the $K_{iz} = 0$ plane. Similar behaviour has been predicted and observed [15] for the x-ray diffuse scattering in the flow-aligned samples of a lyotropic liquid-crystalline hexagonal phase.

The Bragg peaks in the two planes $K_{iz} = \pm C_1$ are turned into Bragg maxima by the thermal fluctuations of the displacement u_z in the columnar direction. In the calculations of the thermal diffuse x-ray scattering intensities, we have omitted the effect of the thermal fluctuations of the displacements in the plane perpendicular to the columns, $u_{q\perp}(\vec{q})$. This is justified since this last quantity has long-range behaviour and would only give a contribution close to the Bragg peaks and not contribute to the long tail behaviour

of the scattered intensities. Along the same lines, we have not considered the diffuse scattering from the internal degrees of freedom of the discotic molecules, i.e. the aliphatic chains for HHTT. We have assumed that such diffuse scattering would not hide the intensity contours predicted here since these degrees of freedom are severely reduced in the ordered columnar phase [5,6]. With the above restrictions, the scattering intensities near the Bragg maxima are shown to have a very anisotropic behaviour in the reciprocal space, with a non-universal behaviour typical of quasi-long-range ordering in the direction of the columns and a long-range behaviour in the basal plane.

Near the Bragg condition for the periodic orientational density, the intensity of the x-ray scattering is predicted to have a very anisotropic power law. In the basal plane, the intensity would decrease with a universal power law $q_{\perp}^{-\frac{1}{2}}$ for $q_z = 0$. The intensity is modulated by the Bessel function of order three as expected for an orientationally ordered state in the columnar direction [16]. This last result washes out the Bragg maxima for $K_{hk} = 0$. In the columnar direction, this decrease would show q_z^{-2} for $q_{\perp} = 0$.

These behaviours near the Bragg maxima lead us to suggest that high intensity and high resolution x-ray scattering measurements should be conducted in order to verify the quasi-long-range behaviour in the orientationally ordered columnar liquid crystal.

VII. ACKNOWLEDGMENTS

We thank M. L. Plumer for early discussions on the simplified model used in this publication. A. L. would like to thank G. Lamoureux for many helpful references. This work was supported by the Natural Sciences and Engineering Research Council of Canada.

APPENDIX : CALCULATION DETAILS

1. Local correlation functions

As explained in section III, aside from terms whose magnitudes scaled with a molecular dimension, the local rms value of the fluctuating variable $u_z(\vec{r})$ is given by :

$$\langle u_z^2(\vec{r}) \rangle = \frac{k_B T}{4\pi\sqrt{KC_1}} \ln \left(\frac{L_\perp}{a} \right), \quad (\text{A1})$$

an expression increasing with the average size L_\perp of the system in a direction perpendicular to the columns with otherwise infinite length.

From (11) and (12) and using the fact that $\Psi(\vec{q})$, $u_z(\vec{q})$ and $u'_{q_\perp}(\vec{q})$ are independent fluctuating quantities, $\langle u_z(\vec{r})\varphi(\vec{r}) \rangle$ is written as :

$$\langle u_z(\vec{r})\varphi(\vec{r}) \rangle = \int \frac{d^3 q}{(2\pi)^3} \left(\frac{a\gamma}{4fg_2} - \frac{b}{2f} \right) \langle |u_z(\vec{q})|^2 \rangle_T. \quad (\text{A2})$$

The bracket appearing in the numerator of the integrand of (A2) has the following long wavelength power expansion :

$$\frac{a\gamma}{4fg_2} - \frac{b}{2f} = \frac{q_\perp^2(Aq_z^2 - Bq_\perp^2)}{Cq_z^4 + Dq_z^2 + E}, \quad (\text{A3})$$

where A and B are constants and C, D , and E are polynomials with only even powers of q_\perp . Looking for the size dependent term, the power expansion (15) is used for $\langle |u_z(\vec{q})|^2 \rangle$, the factor (A3) appearing in the numerator being negative under these conditions, $q_z \ll q_\perp$. As a result, we find that the integrand in (A3) has six simple poles in the complex q_z plane. The three poles located in the upper-half plane are at

$$q_z = \frac{i}{\sqrt{2C}} (D \pm \sqrt{D^2 - 4CE})^{\frac{1}{2}} \quad (\text{A4a})$$

and

$$q_z = i\sqrt{\frac{Kq_\perp^4}{C_1}}. \quad (\text{A4b})$$

The first two poles, in the long wavelength limit, are at :

$$q_z = i\alpha_\pm q_\perp \quad (\text{A5})$$

where $\alpha_{\pm} = (D_0 \pm \sqrt{D_0^2 - 4CE_0})^{1/2}/\sqrt{2C}$ with D_0 and E_0 being two constants depending only on the constants of elasticity A_i, B_i, C_i , and K_i . It is found that only the residue at $q_z = i\sqrt{Kq_{\perp}^4/C_1}$ contribute a term depending on the size of the system. The full integration, in the complex space then gives :

$$\langle u_z(\vec{r})\varphi(\vec{r}) \rangle = -\frac{k_B T}{4\pi\sqrt{KC_1}} \frac{B}{C\alpha_+^2\alpha_-^2} \ln\left(\frac{L_{\perp}}{a}\right) \quad (\text{A6})$$

and, since $B/C\alpha_+^2\alpha_-^2 = B_2/4A_1$, we finally obtain :

$$\langle u_z(\vec{r})\varphi(\vec{r}) \rangle = -\frac{k_B T}{4\pi\sqrt{KC_1}} \frac{B_2}{4A_1} \ln\left(\frac{L_{\perp}}{a}\right). \quad (\text{A7})$$

It has been assumed in the previous calculation that the coefficient of q_{\perp}^2 in

$$D = 8C_5(K_1 + K_2)q_{\perp}^4 + [(16A_2(C_2 + C_3) + 8C_5A_1) - (2B_1 + B_2)^2]q_{\perp}^2 \quad (\text{A8})$$

is positive. It can be easily shown that a negative value for this coefficient would lead to a divergence of the integral in (A2) and therefore to an instability, a possibility that we have rejected from the beginning in the formulation of the model.

Finally, the third local fluctuation correlation function to evaluate is

$$\begin{aligned} \langle \varphi^2(\vec{r}) \rangle = & \int \frac{d^3q}{(2\pi)^3} \left(\langle |\Psi(\vec{q})|^2 \rangle_T + \left(\frac{a\gamma}{4fg_2} - \frac{b}{2f} \right)^2 \langle |u_z(\vec{q})|^2 \rangle_T \right. \\ & \left. + \frac{a^2}{4f^2} \langle |u'_{q\perp}(\vec{q})|^2 \rangle_T \right). \end{aligned} \quad (\text{A9})$$

Each term in the integrand of (A9) is treated separately. The integration of the first term is straightforward and gives :

$$\int \frac{d^3q}{(2\pi)^3} \langle |\Psi(\vec{q})|^2 \rangle_T = \frac{k_B T}{4\pi\sqrt{(K_1 + K_2)A_2}} \ln(K' + \sqrt{K'^2 + 1}) \quad (\text{A10})$$

where $K' = \frac{2\pi}{a} \sqrt{\frac{K_1 + K_2}{A_1}}$. An interesting feature of this result is that it is independent of the size of the system, a result typical of long-range ordering. The second term in the integrand of (A9) is evaluated by following a procedure similar to the one used for (A2), except that the poles (A4a) are now double poles. The result is found to be :

$$\int \frac{d^3q}{(2\pi)^3} \left(\frac{a\gamma}{4fg_2} - \frac{b}{2f} \right)^2 \langle |u_z(\vec{q})|^2 \rangle_T = \frac{k_B T}{4\pi\sqrt{KC_1}} \frac{B_2^2}{16A_1^2} \ln\left(\frac{L_{\perp}}{a}\right). \quad (\text{A11})$$

As for (A2), we have assumed here that the elasticity constants are such that no singularity will appear in the integrand. Finally, the third term in (A9) is also treated with the help of the residue theorem. Writing

$$\int \frac{d^3 q}{(2\pi)^3} \frac{a^2}{4f^2} \langle |u'_{q\perp}(\vec{q})|^2 \rangle_T = k_B T \int \frac{d^3 q}{(2\pi)^3} \frac{a^2}{f(4fg_2)} \quad (\text{A12})$$

with the help of (15), we see upon comparison with (A2) that the locations of the first two poles in the upper-half plane are the same as those given in (A5). The location of the third one, however, is given by the condition $f = 0$,

or

$$q_z = iq_\perp \sqrt{\frac{A_1 + (K_1 + K_2)q_\perp^2}{A_2}} \simeq iq_\perp \sqrt{\frac{A_1}{A_2}} \quad (\text{A13})$$

for small values of q_\perp . The three residues contribute equally to the integral over q_\perp , leading to

$$\int \frac{d^3 q}{(2\pi)^3} \frac{a^2}{4f^2} \langle |u'_{q\perp}(\vec{q})|^2 \rangle_T = \frac{k_B T}{a} \frac{(B_1 + B_2)^2}{A_2^2 C_5} C' \quad (\text{A14})$$

where

$$\begin{aligned} C' = & \frac{\alpha_+}{(\alpha_+^2 + \alpha_-^2)(\alpha_+^2 - \frac{A_1}{A_2})} + \frac{\alpha_-}{(\alpha_-^2 + \alpha_+^2)(\alpha_-^2 - \frac{A_1}{A_2})} \\ & + \frac{\sqrt{\frac{A_1}{A_2}}}{(\frac{A_1}{A_2} + \alpha_-^2)(\frac{A_1}{A_2} - \alpha_+^2)}. \end{aligned} \quad (\text{A15})$$

Again, as in the case of the first term (see eq. (A10)), the result does not depend on the size of the sample. Finally, putting together (A10), (A11) and (A14), we get :

$$\begin{aligned} \langle \varphi^2(\vec{r}) \rangle = & \frac{k_B T}{4\pi \sqrt{(K_1 + K_2)A_2}} \ln(K' + \sqrt{K'^2 + 1}) + \frac{k_B T}{4\pi \sqrt{KC_1}} \frac{B_2^2}{16A_1^2} \ln\left(\frac{L_\perp}{a}\right) \\ & + C' \frac{k_B T}{a} \frac{(B_1 + B_2)^2}{A_2^2 C_5} \end{aligned} \quad (\text{A16})$$

as presented in (19).

2. Correlation functions along the columns

The correlation function $\langle u_z(\vec{r})u_z(\vec{r}') \rangle$ at large distances along the columns (ie $|z - z'| \gg c$ and $|\rho - \rho'|$ of the order of a), after an integration on the angular part in the q_\perp plane, is given by :

$$\langle u_z(\vec{r})u_z(\vec{r}') \rangle = \frac{k_B T}{(2\pi)^2 C_1} \int_{\frac{2\pi}{L_\perp}}^{\frac{2\pi}{a}} dq_\perp q_\perp J_0(q_\perp(\rho - \rho')) \int_{-\infty}^{\infty} dq_z \frac{e^{-iq_z(z-z')}}{q_z^2 + \beta^2 q_\perp^4}. \quad (\text{A17})$$

where J_0 is the Bessel function of order 0 and $\beta = \sqrt{K/C_1}$ ($\vec{\rho}$ and $\vec{\rho}'$ have both been taken parallel to \hat{q}_x for convenience). The integral over q_z can be performed using the residue theorem, keeping only the simple pole located at $q_z = i\beta q_\perp^2$, leading to

$$\langle u_z(\vec{r})u_z(\vec{r}') \rangle = \frac{k_B T}{4\pi\alpha C_1} \int_{\frac{2\pi}{L_\perp}}^{\frac{2\pi}{a}} dq_\perp \frac{J_0(q_\perp(\rho - \rho'))}{q_\perp} e^{-\beta q_\perp^2 |z-z'|}. \quad (\text{A18})$$

This integral is easily performed to give

$$\langle u_z(\vec{r})u_z(\vec{r}') \rangle = \frac{-k_B T}{8\pi\sqrt{KC_1}} \left[2\gamma + E_1\left(\frac{(\rho - \rho')^2}{4\beta|z - z'|}\right) + \ln\left(\frac{\pi^2(\rho - \rho')^2}{L_\perp^2}\right) \right] \quad (\text{A19})$$

where γ is the Euler constant ($\gamma = 0, 57721\dots$) and $E_1(x)$ is the exponential integral function $E_1(x) = \int_x^\infty (e^{-t}/t) dt$.

The second expression of interest to evaluate is $\langle u_z(\vec{r})\varphi(\vec{r}') \rangle$. Using again the same technique applied in (A2), we have :

$$\langle u_z(\vec{r})\varphi(\vec{r}') \rangle = \int \frac{d^3 q}{(2\pi)^3} \left(\frac{a\gamma}{4f g_2} - \frac{b}{2f} \right) \langle |u_z(\vec{q})|^2 \rangle_T e^{-i\vec{q} \cdot (\vec{r} - \vec{r}')}. \quad (\text{A20})$$

The procedure used to evaluate the integral (A20) is practically the same as the one used for $\langle u_z(\vec{r})u_z(\vec{r}') \rangle$, except that we now have three poles when integrating over q_z : $q_z = -i(D \pm \sqrt{D^2 - 4CE})^{\frac{1}{2}}/\sqrt{2C}$, and $q_z = -i\sqrt{Kq_\perp^4/C_1}$. As in the calculation of $\langle u_z(\vec{r})\varphi(\vec{r}) \rangle$, the only significative contribution to the integral comes from the residue at $q_z = -i\sqrt{Kq_\perp^4/C_1}$, and we have to evaluate

$$\langle u_z(\vec{r})\varphi(\vec{r}') \rangle = -\frac{k_B T}{4\pi\alpha C_1} \frac{B}{C\alpha_+^2 \alpha_-^2} \int_{\frac{2\pi}{L_\perp}}^{\frac{2\pi}{a}} dq_\perp \frac{J_0(q_\perp(\rho - \rho'))}{q_\perp} e^{-\beta q_\perp^2 |z-z'|}, \quad (\text{A21})$$

an integral which is identical to the one in (A18). The final result is then :

$$\begin{aligned} \langle u_z(\vec{r})\varphi(\vec{r}') \rangle = & \frac{k_B T}{8\pi\sqrt{KC_1}} \frac{B_2}{4A_1} \left[2\gamma + E_1\left(\frac{(\rho - \rho')^2}{4\beta|z - z'|}\right) \right. \\ & \left. + \ln\left(\frac{\pi^2(\rho - \rho')^2}{L_\perp^2}\right) \right]. \end{aligned} \quad (\text{A22})$$

The last expression to evaluate is $\langle \varphi(\vec{r})\varphi(\vec{r}') \rangle$ which is written as :

$$\langle \varphi(\vec{r})\varphi(\vec{r}') \rangle = I_1 + I_2 + I_3, \quad (\text{A23})$$

where

$$I_1 = \int \frac{d^3 q}{(2\pi)^3} \langle |\Psi(\vec{q})|^2 \rangle_T e^{-i\vec{q} \cdot (\vec{r} - \vec{r}')} , \quad (\text{A24a})$$

$$I_2 = \int \frac{d^3 q}{(2\pi)^3} \left(\frac{a\gamma}{4fg_2} - \frac{b}{2f} \right)^2 \langle |u_z(\vec{q})|^2 \rangle_T e^{-i\vec{q} \cdot (\vec{r} - \vec{r}')} , \quad (\text{A24b})$$

and

$$I_3 = \int \frac{d^3 q}{(2\pi)^3} \frac{a^2}{4f^2} \langle |u'_{q_\perp}(\vec{q})|^2 \rangle_T e^{-i\vec{q} \cdot (\vec{r} - \vec{r}')} . \quad (\text{A24c})$$

After a first integration on the angular part in the q_\perp -plane, I_1 becomes

$$I_1 = \frac{k_B T}{(2\pi)^2 A_2} \int_{\frac{2\pi}{L_\perp}}^{\frac{2\pi}{a}} dq_\perp q_\perp J_0(q_\perp(\rho - \rho')) \int_{-\infty}^{\infty} dq_z \frac{e^{-iq_z(z - z')}}{q_z^2 + \eta_1 q_\perp^2 + \eta_2 q_\perp^4} \quad (\text{A25})$$

where $\eta_1 = A_1/A_2$ and $\eta_2 = (K_1 + K_2)/A_2$. Keeping only the simple pole at $q_z = -i\sqrt{\eta_1}q_\perp$ (since again the integrand is dominated by small values of q_\perp), we obtain :

$$I_1 = \frac{k_B T}{4\pi A_2 \sqrt{\eta_1}} \int_{\frac{2\pi}{L_\perp}}^{\frac{2\pi}{a}} dq_\perp q_\perp J_0(q_\perp(\rho - \rho')) e^{-\sqrt{\eta_1}q_\perp|z - z'|} . \quad (\text{A26})$$

After performing a change of variable $y = \sqrt{\eta_1}|z - z'|q_\perp$, using the power series $J_0(x) = \sum_{k=0}^{\infty} (-1)^k (x/2)^{2k}/k! \Gamma(k+1)$ and the function $\Gamma(n) = (n-1)! = \int_0^{\infty} t^{n-1} e^{-t} dt$ (for $n > 0$), we have :

$$I_1 = \frac{k_B T}{4\pi A_2 \sqrt{\eta_1}} \frac{1}{|z - z'| \sqrt{\eta_1}} \sum_{k=0}^{\infty} \frac{(2k)!}{(k!)^2} \left(\frac{-(\rho - \rho')^2}{4\eta_1(z - z')^2} \right)^k . \quad (\text{A27})$$

Finally, since $\sum_{k=0}^{\infty} (-x)^k (2k)!/(k!)^2 = 1/\sqrt{1+4x}$, we obtain

$$I_1 = \frac{k_B T}{8\pi} \frac{\xi_1}{\sqrt{\kappa_1(z-z')^2 + (\rho-\rho')^2}} \quad (\text{A28})$$

with $\xi_1 = 2/\sqrt{A_1 A_2}$ and $\kappa_1 = \eta_1 = A_1/A_2$.

The calculation of I_2 is similar to the one for $\langle u_z(\vec{r})\varphi(\vec{r}') \rangle$. Since the integrand now has two double poles at $q_z = -i(D \pm \sqrt{D^2 - 4CE})^{1/2}/\sqrt{2C}$, the only significant contribution originates from the residue at $q_z = -i\sqrt{Kq_\perp^4/C_1}$.

Thus we easily find, upon comparison with (A20), that

$$I_2 = -\frac{k_B T}{8\pi\sqrt{KC_1}} \left(\frac{B_2}{4A_1} \right)^2 \left[2\gamma + E_1 \left(\frac{(\rho-\rho')^2}{4\beta|z-z'|} \right) + \ln \left(\frac{\pi^2(\rho-\rho')^2}{L_\perp^2} \right) \right]. \quad (\text{A29})$$

Finally, after an integration over the angular contribution in the q_\perp -plane, I_3 yields

$$\begin{aligned} I_3 = & \frac{k_B T}{(2\pi)^2} \frac{(B_1 + \frac{1}{2}B_2)^2}{4} \int_{\frac{2\pi}{L_\perp}}^{\frac{2\pi}{a}} dq_\perp q_\perp^3 J_0(q_\perp(\rho-\rho')) \\ & \times \int_{-\infty}^{\infty} dq_z q_z^2 \frac{e^{-iq_z(z-z')}}{(Cq_z^4 + Dq_z^2 + E)f} \end{aligned} \quad (\text{A30})$$

where C , D and E are the same functions as those defined in (A3). As found previously in the development of the third term in the integrand of (A9), the integrand of I_3 has four simple poles at $q_z = \pm i\alpha_\pm q_\perp$ and the condition $f = 0$ yields two more simple poles at $q_z = \pm i\sqrt{A_1/A_2}q_\perp$. We finally find, after an integration over q_\perp ,

$$I_3 = \frac{k_B T}{8\pi} \sum_{i=2}^4 \frac{\xi_i}{\sqrt{\kappa_i(z-z')^2 + (\rho-\rho')^2}} \quad (\text{A31})$$

with the following definitions :

$$\xi_2 = \frac{-(B_1 + \frac{1}{2}B_2)^2 \alpha_+}{(\alpha_+^2 - \alpha_-^2)(\alpha_+^2 - \frac{A_1}{A_2})}, \quad (\text{A32a})$$

$$\xi_3 = \frac{-(B_1 + \frac{1}{2}B_2)^2 \alpha_-}{(\alpha_-^2 - \alpha_+^2)(\alpha_-^2 - \frac{A_1}{A_2})}, \quad (\text{A32b})$$

$$\xi_4 = \frac{-(B_1 + \frac{1}{2}B_2)^2 \sqrt{\frac{A_1}{A_2}}}{(\frac{A_1}{A_2} - \alpha_-^2)(\frac{A_1}{A_2} - \alpha_+^2)}, \quad (\text{A32c})$$

and $\kappa_2 = \alpha_+^2$, $\kappa_3 = \alpha_-^2$, and $\kappa_4 = A_1/A_2$. It is found numerically that the value of I_3 is positive for $|z - z'| \gg c$ and $|\rho - \rho'| \simeq a$, which is precisely the limit used for the present calculations.

Thus combining (A28), (A29) and (A31), we obtain :

$$\begin{aligned} \langle \varphi(\vec{r})\varphi(\vec{r}') \rangle = & \frac{k_B T}{8\pi} \sum_{i=1}^4 \frac{\xi_i}{\sqrt{\kappa_i(z-z')^2 + (\rho-\rho')^2}} \\ & - \frac{k_B T}{8\pi\sqrt{KC_1}} \frac{B_2^2}{16A_1^2} \left[2\gamma + E_1\left(\frac{(\rho-\rho')^2}{4\beta|z-z'|}\right) \right. \\ & \left. + \ln\left(\frac{\pi^2(\rho-\rho')^2}{L_\perp^2}\right) \right] \end{aligned} \quad (\text{A33})$$

as presented in (23).

3. Correlation functions in the plane perpendicular to the columnar direction

The correlations at large distances in the plane perpendicular to the columnar direction, ie $|z - z'| \ll c$ and $|\rho - \rho'| \gg a$ are easily obtained. Indeed, referring to (20), they are dominated by small values of q_\perp and an integration over all values of q_z . The limit $q_z \gg q_\perp$ is then justified. From the denominator expression (14), the correlation functions are anticipated to have a behaviour typical of long-range ordering. Expressions having a structure similar to (A28) are then obtained as expected for random fluctuations for long-range ordering.

For example, the value of $\langle u_z(\vec{r})u_z(\vec{r}') \rangle$ is explicitly given by :

$$\langle u_z(\vec{r})u_z(\vec{r}') \rangle = \frac{k_B T}{C_1(2\pi)^2} \int_{\frac{2\pi}{L_\perp}}^{\frac{2\pi}{a}} q_\perp J_0(q_\perp\rho) dq_\perp \int_{-\infty}^{\infty} dq_z \frac{e^{-iq_z z}}{q_z^2 + \beta^2 q_\perp^2} \quad (\text{A34})$$

where $\beta = \sqrt{G/C_1}$. The integrations are easily performed and yield

$$\langle u_z(\vec{r})u_z(\vec{r}') \rangle = \frac{k_B T}{4\pi\sqrt{KC_1}} \frac{1}{\sqrt{\alpha^2(z-z')^2 + (\rho-\rho')^2}}, \quad (\text{A35})$$

an expression having a structure similar to (A28). The results for $\langle u_z(\vec{r})\varphi(\vec{r}') \rangle$ and $\langle \varphi(\vec{r})\varphi(\vec{r}') \rangle$ give similar structures.

4. Density-density correlation function in the columnar direction

In this section, we present the calculations performed to evaluate explicitly the function

$$\begin{aligned} G(\vec{r} - \vec{r}') = & \langle \rho_c(\vec{r}) \rho_c(\vec{r}') \rangle + \langle \rho_c(\vec{r}) \rho_g(\vec{r}') \rangle \\ & + \langle \rho_g(\vec{r}) \rho_c(\vec{r}') \rangle + \langle \rho_g(\vec{r}) \rho_g(\vec{r}') \rangle. \end{aligned} \quad (\text{A36})$$

The first term in (A36) is explicitly given by

$$\begin{aligned} \langle \rho_c(\vec{r}) \rho_c(\vec{r}') \rangle = & \sum_i \sum_{i'} b_{\vec{K}_i} b_{\vec{K}_{i'}} \langle \cos(K_{i\perp} \rho \cos \alpha + K_{iz}(z - u_z(\vec{r}))) \\ & \times \cos(K_{i'\perp} \rho' \cos \alpha + K_{i'z}(z' - u_z(\vec{r}'))) \rangle. \end{aligned} \quad (\text{A37})$$

$\vec{\rho}$ and $\vec{\rho}'$ have been taken parallel. Using the property $\langle \exp[\alpha_i x_i] \rangle_T = \exp[\alpha_i \alpha_k \langle x_i x_k \rangle_T / 2]$, (A37) becomes :

$$\begin{aligned} \langle \rho_c(\vec{r}) \rho_c(\vec{r}') \rangle = & \frac{1}{4} \sum_i \sum_{i'} \left[F_1 \exp \left[- \left((K_{iz}^2 + K_{i'z}^2) \langle u_z^2(\vec{r}) \rangle \right. \right. \right. \\ & \left. \left. \left. + 2K_{iz}K_{i'z} \langle u_z(\vec{r}) u_z(\vec{r}') \rangle \right) \right] \\ & + F_2 \exp \left[- \left((K_{iz}^2 + K_{i'z}^2) \langle u_z^2(\vec{r}) \rangle \right. \right. \\ & \left. \left. - 2K_{iz}K_{i'z} \langle u_z(\vec{r}) u_z(\vec{r}') \rangle \right) \right], \end{aligned} \quad (\text{A38})$$

where $F_1 = 2b_{\vec{K}_i} b_{\vec{K}_{i'}} \cos(\vec{K}_i \cdot \vec{r} + \vec{K}_{i'} \cdot \vec{r}')$ and $F_2 = 2b_{\vec{K}_i} b_{\vec{K}_{i'}} \cos(\vec{K}_i \cdot \vec{r} - \vec{K}_{i'} \cdot \vec{r}')$. After substitution of (17) and (A19) in (A38), we find that $\langle \rho_c(\vec{r}) \rho_c(\vec{r}') \rangle$ depends only on $|\vec{r} - \vec{r}'|$ (and consequently is independent of L_\perp) if and only if $\vec{K}_i = -\vec{K}_{i'}$ (for the first term in (A38)) or $\vec{K}_i = \vec{K}_{i'}$ (for the second term in (A38)). This condition is required by the overall translational invariance

of the system. Consequently, we find

$$\begin{aligned} \langle \rho_c(\vec{r})\rho_c(\vec{r}') \rangle = & \frac{1}{2} \sum_i \sum_{i'} b_{\vec{K}_i} b_{\vec{K}_{i'}} \left[\cos(\vec{K}_i \cdot \vec{r} + \vec{K}_{i'} \cdot \vec{r}') \delta_{\vec{K}_i, -\vec{K}_{i'}} \right. \\ & + \cos(\vec{K}_i \cdot \vec{r} - \vec{K}_{i'} \cdot \vec{r}') \delta_{\vec{K}_i, \vec{K}_{i'}} \Big] \\ & \times \exp \left[-X(K_{iz}) \left(2\gamma + E_1 \left(\frac{(\rho - \rho')^2}{4\beta|z - z'|} \right) \right) \right] \\ & \times \left(\frac{a}{\pi|\rho - \rho'|} \right)^{2X(K_{iz})}, \end{aligned} \quad (\text{A39})$$

or, using the development $E_1(x) \simeq -\gamma - \ln(x)$ for $x \ll 1$,

$$\langle \rho_c(\vec{r})\rho_c(\vec{r}') \rangle \sim \sum_i b_{\vec{K}_i}^2 \cos \vec{K}_i \cdot (\vec{r} - \vec{r}') \left(\frac{a^2}{4\pi^2\beta|z - z'|} \right)^{X(K_{iz})}, \quad (\text{A40})$$

where $X(K_{iz}) = K_{iz}^2 \frac{k_B T}{8\pi\sqrt{KC_1}}$.

The second term in (24) is given by

$$\begin{aligned} \langle \rho_c(\vec{r})\rho_g(\vec{r}') \rangle = & \frac{\rho_{g0}}{4} \sum_i \sum_{n', m'} \sum_{j'=0}^2 b_{\vec{K}_i} \delta(\vec{p}' - (\vec{p}_{n'm'} + \vec{p}_{j'} + \vec{\sigma}')) \\ & \times \langle \cos(K_{i\perp}\rho \cos(\alpha_\perp - \alpha_i) + K_{iz}(z - u_z(\vec{r}))) \\ & \times \cos 3(\theta' - H_{j'}\omega(z' - u_z(\vec{r}')) \\ & - (\Omega_{j'} - \varphi(\vec{r}')) \rangle. \end{aligned} \quad (\text{A41})$$

It can be written, with the help of (25), as

$$\begin{aligned} \langle \rho_c(\vec{r})\rho_g(\vec{r}') \rangle = & \rho_{g0} \sum_i \sum_{n', m'} \sum_{j'=0}^2 \left[F_1 \exp \left(-\frac{1}{2}U_1 \right) \right. \\ & \left. + F_2 \exp \left(-\frac{1}{2}U_2 \right) \right], \end{aligned} \quad (\text{A42})$$

where

$$\begin{aligned} U_1 = & (K_{iz}^2 + 9\omega^2)\langle u_z^2(\vec{r}) \rangle + 9\langle \varphi^2(\vec{r}) \rangle - 6K_{iz}H_{j'}\omega\langle u_z(\vec{r})u_z(\vec{r}') \rangle \\ & - 6K_{iz}\langle u_z(\vec{r})\varphi(\vec{r}') \rangle + 18H_{j'}\omega\langle u_z(\vec{r}')\varphi(\vec{r}') \rangle, \end{aligned} \quad (\text{A43a})$$

$$\begin{aligned} U_2 = & (K_{iz}^2 + 9\omega^2)\langle u_z^2(\vec{r}) \rangle + 9\langle \varphi^2(\vec{r}) \rangle + 6K_{iz}H_{j'}\omega\langle u_z(\vec{r})u_z(\vec{r}') \rangle \\ & + 6K_{iz}\langle u_z(\vec{r})\varphi(\vec{r}') \rangle + 18H_{j'}\omega\langle u_z(\vec{r}')\varphi(\vec{r}') \rangle, \end{aligned} \quad (\text{A43b})$$

$$F_1 = 2b_{\vec{K}_i}\delta(\vec{\rho}' - (\vec{\rho}_{n'm'} + \vec{\rho}_{j'} + \vec{\sigma}')) \cos(\vec{K}_i \cdot \vec{r} - 3(-\theta' + H_{j'}\omega z' + \Omega_{j'})), \quad (\text{A44a})$$

$$F_2 = 2b_{\vec{K}_i}\delta(\vec{\rho}' - (\vec{\rho}_{n'm'} + \vec{\rho}_{j'} + \vec{\sigma}')) \cos(\vec{K}_i \cdot \vec{r} + 3(-\theta' + H_{j'}\omega z' + \Omega_{j'})). \quad (\text{A44b})$$

Substituting (17), (A7), (A16), (A19) and (A22) into (A43), we find that (A42) depends on $|\vec{r} - \vec{r}'|$ if and only if

$$K_{iz} = \pm 3 \left(H_j\omega - \frac{B_2}{4A_1} \right). \quad (\text{A45})$$

Rewriting (A16) as

$$\langle \varphi^2(\vec{r}) \rangle = F_0 + \frac{k_B T}{4\pi\sqrt{KC_1}} \frac{B_2^2}{16A_1^2} \ln \left(\frac{L_\perp}{a} \right) \quad (\text{A46})$$

where

$$\begin{aligned} F_0 = & \frac{k_B T}{4\pi\sqrt{(K_1 + K_2)A_2}} \ln(K' + \sqrt{K'^2 + 1}) \left(\frac{L_\perp}{a} \right) \\ & - C' \frac{k_B T}{a} \frac{(B_1 + B_2)^2}{A_2^2 C_5}, \end{aligned} \quad (\text{A47})$$

we finally find

$$\begin{aligned} \langle \rho_g(\vec{r})\rho_c(\vec{r}') \rangle = & \frac{\rho_{g0}}{4} \sum_i \sum_{n',m'} \sum_{j'=0}^2 (F_1 + F_2) \\ & \times \exp \left[-X'_{j'} \left(2\gamma + E_1 \left(\frac{(\rho - \rho')^2}{4\beta|z - z'|} \right) \right) - \frac{9}{2}F_0 \right] \\ & \times \left(\frac{a}{\pi|\rho - \rho'|} \right)^{X'_{j'}} \delta_{K_{iz}, \pm 3 \left(H_j\omega - \frac{B_2}{4A_1} \right)}, \end{aligned} \quad (\text{A48})$$

where

$$X'_{j'} = \frac{9k_B T}{8\pi\sqrt{KC_1}} \left(H_j\omega - \left(\frac{B_2}{4A_1} \right) \right)^2. \quad (\text{A49})$$

The third term in (24), $\langle \rho_g(\vec{r})\rho_c(\vec{r}') \rangle$, is obtained exactly like the second one, and the result is identical to (A48), with the changes $i \rightarrow i'$, $n' \rightarrow n$, $m' \rightarrow m$, and $j' \rightarrow j$. Finally, the fourth term in (24) can be explicitly written

as

$$\begin{aligned}
\langle \rho_g(\vec{r}) \rho_g(\vec{r}') \rangle = & \rho_{g0}^2 \sum_{n,m} \sum_{n',m'} \sum_{j=0}^2 \sum_{j'=0}^2 \delta(\vec{\rho} - (\vec{\rho}_{nm} + \vec{\rho}_j + \vec{\sigma})) \\
& \times \delta(\vec{\rho}' - (\vec{\rho}_{n'm'} + \vec{\rho}_{j'} + \vec{\sigma}')) \\
& \times \langle \cos 3(\theta - H_j \omega(z - u_z(\vec{r})) - (\Omega_j - \varphi(\vec{r}))) \\
& \times \cos 3(\theta' - H_{j'} \omega(z' - u_z(\vec{r}')) \\
& - (\Omega_{j'} - \varphi(\vec{r}')) \rangle. \tag{A50}
\end{aligned}$$

Using the property (25), we find

$$\begin{aligned}
\langle \rho_g(\vec{r}) \rho_g(\vec{r}') \rangle = & \frac{\rho_{g0}^2}{4} \sum_{n,m} \sum_{n',m'} \sum_{j=0}^2 \sum_{j'=0}^2 \left[F_1 \exp \left(-\frac{1}{2} U_1 \right) \right. \\
& \left. + F_2 \exp \left(-\frac{1}{2} U_2 \right) \right], \tag{A51}
\end{aligned}$$

where

$$\begin{aligned}
U_1 = & 18 \left[\omega^2 \langle u_z^2(\vec{r}) \rangle + \langle \varphi^2(\vec{r}) \rangle + H_j H_{j'} \omega^2 \langle u_z(\vec{r}) u_z(\vec{r}') \rangle \right. \\
& + H_j \omega \left(\langle u_z(\vec{r}) \varphi(\vec{r}') \rangle + \langle u_z(\vec{r}) \varphi(\vec{r}) \rangle \right) \\
& + H_{j'} \omega \left(\langle \varphi(\vec{r}) u_z(\vec{r}') \rangle + \langle \varphi(\vec{r}') u_z(\vec{r}') \rangle \right) \\
& \left. + \langle \varphi(\vec{r}) \varphi(\vec{r}') \rangle \right], \tag{A52a}
\end{aligned}$$

$$\begin{aligned}
U_2 = & 18 \left[\omega^2 \langle u_z^2(\vec{r}) \rangle + \langle \varphi^2(\vec{r}) \rangle - H_j H_{j'} \omega^2 \langle u_z(\vec{r}) u_z(\vec{r}') \rangle \right. \\
& + H_j \omega \left(- \langle u_z(\vec{r}) \varphi(\vec{r}') \rangle + \langle u_z(\vec{r}) \varphi(\vec{r}) \rangle \right) \\
& + H_{j'} \omega \left(- \langle \varphi(\vec{r}) u_z(\vec{r}') \rangle + \langle \varphi(\vec{r}') u_z(\vec{r}') \rangle \right) \\
& \left. - \langle \varphi(\vec{r}) \varphi(\vec{r}') \rangle \right], \tag{A52b}
\end{aligned}$$

$$\begin{aligned}
F_1 = & \delta(\vec{\rho} - (\vec{\rho}_{nm} + \vec{\rho}_j + \vec{\sigma})) \delta(\vec{\rho}' - (\vec{\rho}_{n'm'} + \vec{\rho}_{j'} + \vec{\sigma}')) \\
& \times \cos 3(\theta - H_j \omega z - \Omega_j + (\theta' - H_{j'} \omega z' - \Omega_{j'})), \tag{A53a}
\end{aligned}$$

and

$$\begin{aligned} F_2 = & \delta(\vec{\rho} - (\vec{\rho}_{nm} + \vec{\rho}_j + \vec{\sigma}))\delta(\vec{\rho}' - (\vec{\rho}_{n'm'} + \vec{\rho}_{j'} + \vec{\sigma}')) \\ & \times \cos 3(\theta - H_j \omega z - \Omega_j - (\theta' - H_{j'} \omega z' - \Omega_{j'})). \end{aligned} \quad (\text{A53b})$$

As before, we substitute (17), (A7), (A16), (A19), (A22) and (A33) into (A43). Then we evaluate, for both cases $H_j = H_{j'}$ and $H_j = -H_{j'}$, the conditions under which U_1 and U_2 will depend on $|\vec{r} - \vec{r}'|$. It is found that U_1 meets this requirement when $H_j = H_{j'} = 1$ and $\omega = B_2/4A_1$, a condition which is too restrictive. However, U_2 meets this requirement provided $H_j = H_{j'}$. Effectively, under this last condition, we have

$$U_2 = 2X'_j \left[2\gamma + E_1 \left(\frac{(\rho - \rho')^2}{4\beta|z - z'|} \right) + \ln \left(\frac{\pi^2(\rho - \rho')^2}{a^2} \right) \right] - 9F(\vec{r} - \vec{r}') \quad (\text{A54})$$

where

$$F(\vec{r} - \vec{r}') = \frac{k_B T}{8\pi} \sum_{i=1}^4 \frac{\xi_i}{\sqrt{\kappa_i(z - z')^2 + (\rho - \rho')^2}} + F_0, \quad (\text{A55})$$

and X'_j is given by (A49). The final result for the fourth term of (24) is

$$\langle \rho_g(\vec{r})\rho_g(\vec{r}') \rangle = \frac{\rho_{g0}^2}{4} \sum_{n,m} \sum_{n',m'} \sum_{j=0}^2 \sum_{j'=0}^2 F_2 \exp \left(-\frac{1}{2} U_2 \right), \quad (\text{A56})$$

with the function U_2 given in (A54) or, using again the development $E_1(x) \simeq -\gamma - \ln(x)$ for $x \ll 1$ and the fact that $F(\vec{r} - \vec{r}') \simeq F_0$ for large distances,

$$\langle \rho_g(\vec{r})\rho_g(\vec{r}') \rangle \sim \sum_{j=0}^2 F_2 \left(\frac{a^2}{4\pi^2\beta|z - z'|} \right)^{X'_j}. \quad (\text{A57})$$

5. Scattered intensity calculations

This section presents the calculations pertaining to the thermal diffuse scattering near the Bragg condition due to the periodic orientation density for $q_z \simeq 0$ and $q_\perp \gg q_z$. As mentioned in the text, the effect of the thermal diffuse scattering near these Bragg conditions is calculated from $I_{gg}(\vec{Q})$, which is evaluated by taking $\vec{r}' = \vec{\rho}_{j'} + \vec{\sigma}'$ (ie $\vec{\rho}_{n'm'} = \vec{0}$ and $z' = 0$) for a momentum

transfer $\vec{Q} = \vec{K}_{hk} + \vec{q}_\perp + 3\omega\hat{z} + q_z\hat{z}$, with \vec{q}_\perp and q_z very small on the scale of the inverse of their respective intermolecular dimension. For $q_z = 0$ and $q_\perp \gg q_z$, the integral $I_{gg}(\vec{r})$ is dominated by a cone surrounding the z-axis. After a first integration over the basal xy plane, we obtain

$$\begin{aligned}
 I_{gg}(\vec{Q}) \propto & \sum_{\{j,j'\}} \sum_{nm} \int_{-\infty}^{\infty} dz \int_0^{2\pi} d\theta \int_0^{2\pi} d\theta' \left(\exp[i3\Phi] + \exp[-i3\Phi] \right) \\
 & \times \exp \left[-X'_j \left(2\gamma + E_1 \left(\frac{\rho_{nmj}^2}{4\beta|z|} \right) \right) \right] \left(\frac{a}{\pi\rho_{nmj}} \right)^{2X'_j} \\
 & \times \exp \left[-\frac{9}{2} \left(F_0 + \sum_{i=1}^4 \xi_i (\kappa_i z^2 + \rho_{nmj}^2)^{-1/2} \right) \right] \\
 & \times \exp \left[i(\vec{K}_{hk} + \vec{q}_\perp)(\vec{\rho}_{nmj} + \vec{\sigma} - \vec{\rho}_{j'} - \vec{\sigma}') \right] \\
 & \times \exp \left[i(3\omega + q_z)z \right]
 \end{aligned} \tag{A58}$$

where $\Phi = \theta - \theta' - (\theta_{oj}(z) - \theta_{oj'}(0))$, $\vec{\rho}_{nmj} = \vec{\rho}_{nm} + \vec{\rho}_j$ and $\{j, j'\}$ represents the pairs of indices (j, j') that are such that $H_j = H_{j'}$. The integration over the angular contribution within the columns and the summation over the six given couples (j, j') yields :

$$\begin{aligned}
 I_{gg}(\vec{Q}) \propto & \int_0^{\infty} \rho d\rho \int_{-\infty}^{\infty} dz J_3^2(K_{hk}R_0) \exp[i3q_z z] \\
 & \times \exp \left[-\frac{9}{2} \left(F_0 + \sum_{i=1}^4 \xi_i (\kappa_i z^2 + \rho^2)^{-1/2} \right) \right] \\
 & \times \exp \left[-X'_0 \left(2\gamma + E_1 \left(\frac{\rho^2}{4\beta|z|} \right) \right) \right] \left(\frac{a}{\pi\rho} \right)^{2X'_0} J_0(q_\perp \rho) \\
 & + \int_0^{\infty} \rho d\rho \int_{-\infty}^{\infty} dz J_3^2(K_{hk}R_0) \exp[i3q_z z] \\
 & \times \exp \left[-\frac{9}{2} \left(F_0 + \sum_{i=1}^4 \xi_i (\kappa_i z^2 + \rho^2)^{-1/2} \right) \right] \\
 & \times 2 \exp \left[-X'_1 \left(2\gamma + E_1 \left(\frac{\rho^2}{4\beta|z|} \right) \right) \right] \left(\frac{a}{\pi\rho} \right)^{2X'_1} \\
 & \times \left(1 + \cos(\vec{q}_\perp \cdot (\vec{\rho}_2 - \vec{\rho}_1)) \right) J_0(q_\perp \rho)
 \end{aligned} \tag{A59}$$

where we have neglected $|\vec{\rho}_j|$ in front of $|\vec{\rho}_{nm}|$ and extended the infinite sum over ρ_{nm} to an integral over the continuous variable ρ . With the changes of variables $w = \rho^2/4\beta|z|$ and $z' = 3q_z z$, (A59) can be rewritten as

$$\begin{aligned} I_{gg}(\vec{G}) \propto & \frac{J_3^2(K_{hk}R_0)}{q_z^{2-X'_0}} \int_0^\infty dz' \exp[iz'] z'^{1-X'_0} \int_0^\infty dw w^{-X'_0} \exp[-X'_0 E_1(w)] \\ & \times J_0\left(2q_\perp \sqrt{\frac{w\beta z'}{3q_z}}\right) \prod_{i=1}^4 \exp[-\xi_i(\tau_i z'^2 + \tau' \omega |z'|)^{-1/2}] \\ & + \frac{2J_3^2(K_{hk}R_0)(1 + \cos(\vec{q}_\perp \cdot (\vec{\rho}_2 - \vec{\rho}_1)))}{q_z^{2-X'_1}} \int_0^\infty dz' \exp[iz'] z'^{1-X'_1} \\ & \times \int_0^\infty dw w^{-X'_1} \exp[-X'_1 E_1(w)] \\ & \times J_0\left(2q_\perp \sqrt{\frac{w\beta z'}{3q_z}}\right) \prod_{i=1}^4 \exp[-\xi_i(\tau_i z'^2 + \tau' \omega |z'|)^{-1/2}] \end{aligned} \quad (\text{A60})$$

where $\tau_i = \kappa_i/9q_z^2$ and $\tau' = 4\beta/3|q_z|$, as presented in (42). Using scaling techniques, the two integrals in the first term of (A60) are found to be proportional to $q_z^{2-X'_0}/\sqrt{q_\perp}$, while the two integrals in the second term of (A60) are found to be proportional to $q_z^{2-X'_1}/\sqrt{q_\perp}$, leading to

$$I_{gg}(\vec{Q}) \propto \frac{J_3^2(K_{hk}R_0)}{\sqrt{q_\perp}} (3 + 2 \cos(\vec{q}_\perp \cdot (\vec{\rho}_2 - \vec{\rho}_1))). \quad (\text{A61})$$

REFERENCES

- [1] A. Caillé, C.R. Acad. Sc. Paris B, t. 274, 891 (1972).
- [2] J. Als-Nielsen, R.J. Birgeneau, M. Kaplan, J.D. Litster and C. R. Safinya, Phys. Rev. Lett. **39**, 1668 (1977).
- [3] J. Als-Nielsen, J.D. Litster, R.J. Birgeneau, M. Kaplan, C.R. Safinya, A. Lindegaard-Andersen and S. Mathiesen, Phys. Rev. B **22**, 312 (1980).
- [4] P.-G. de Gennes and J. Prost, The physics of liquid crystals (2nd edition), Oxford University Press, New York (1993).
- [5] E. Fontes, P. A. Heiney and W. H. de Jeu, Phys. Rev. Lett. **61**, 1202 (1988).
- [6] P. A. Heiney, E. Fontes, W. H. de Jeu, A. Riera, P. Carroll and A. B. Smith, III, J. Phys. (France) **50**, 461 (1989).
- [7] A. M. Levelut, J. Phys. (France) Lett. **40**, L81 (1979).
- [8] S. Chandrasekhar and G. S. Ranganath, Rep. Prog. Phys. **53**, 57 (1990).
- [9] H. R. Brand and H. Pleiner, Phys. Rev. Lett. **69**, 987 (1992).
- [10] G. Durand, Phys. Rev. Lett. **69**, 988 (1992).
- [11] A. Caillé and Mathieu Hébert, Phys. Rev. E **54**, R4544 (1996).
- [12] L. Landau and E. Lifshitz, Statistical physics, Part 1 (3rd edition), Pergamon Press, New York (1980).
- [13] S. Idziak, Ph.D. dissertation, University of Pennsylvania (1989).
- [14] P. Davidson, M. Clerc, S. S. Ghosh, N. C. Maliszewskyj, P.A. Heiney, J. Hynes Jr. and A. B. Smith, III, J. Phys II (France) **5**, 249 (1995).
- [15] M. Impérator-Clerc and P. Davidson, Eur. Phys. J., **B9**, 93 (1999).
- [16] J. D. Watson and F. H. C. Crick, Nature **171**, 737 (1953).

Figure Captions

- Fig. 1 a) Top view of the two-dimensional columnar structure, the full black dots (labeled 1 and 2) being the displaced columns and the open dots (labeled 0), the undisplaced columns. b) Three dimensional side view of the molecular stacks in three different columns in their equilibrium configurations if long-range ordering is assumed.
- Fig. 2 The equilibrium core density continuum (a) at $z = 0$ in the basal plane; (b) at $z = c/2$ in the basal plane; (c) at $(x, y) = (0, 0)$ and $(x, y) = (a, 0)$ as a function of z . In Fig. 2(a) and 2(b), the unit cell is represented schematically showing the presence of maxima at the corner of the cell in Fig 2(a) and two maxima inside the cell on Fig 2(b). Arbitrary values have been used ($a = 10$, $c = 4$ and the coefficients b_2 to b_{10} were all set to unity). x and y have the same units as a , z have the same units as c and ρ has the same units as ρ_0 and b_{K_i} .
- Fig. 3 Groove density modulation $(1 - \rho_{g0}(z, \theta))$ along a continuous column of stacked molecules. Arbitrary values have been used ($\rho_0 = 1$, $c = 4$, $H_j = 1$ and $\Omega_j = 0$). z has the same units as c .
- Fig. 4 Representation of the vectors \vec{r} , $\vec{\rho}$ and $\vec{\sigma}$ used to locate a point on the surface of molecular cylinders.

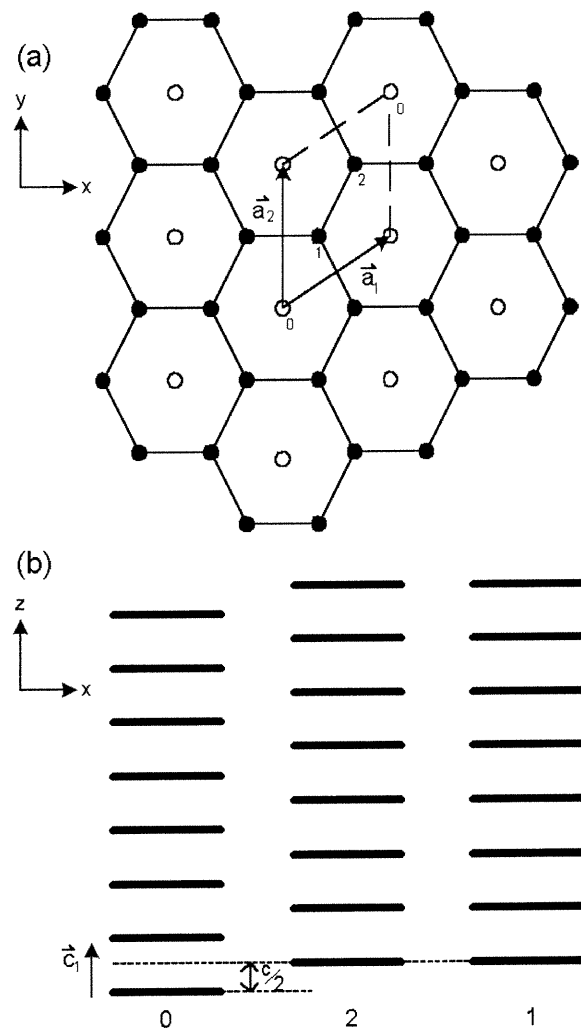


Figure 1

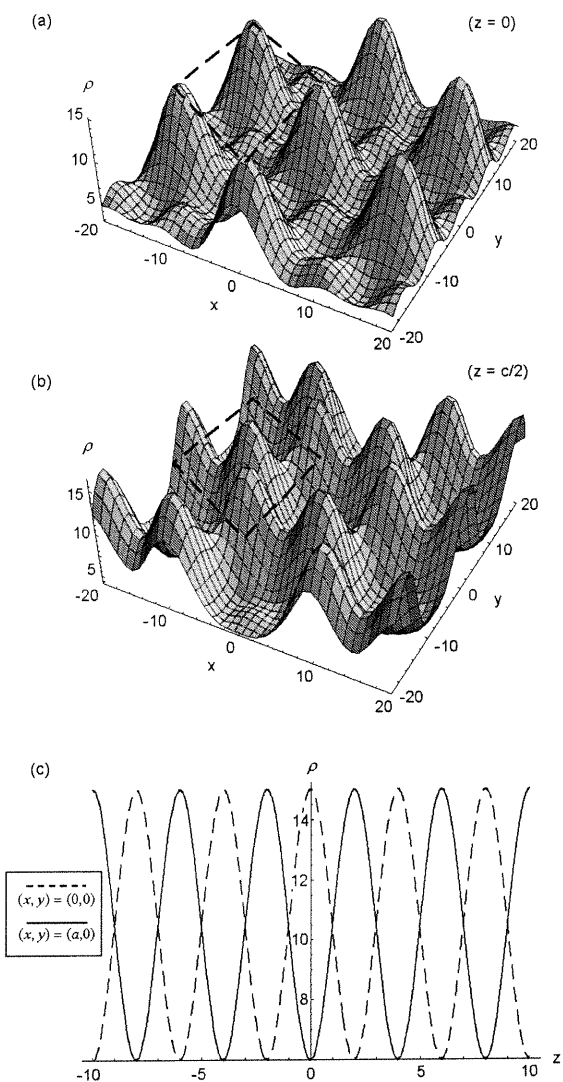


Figure 2

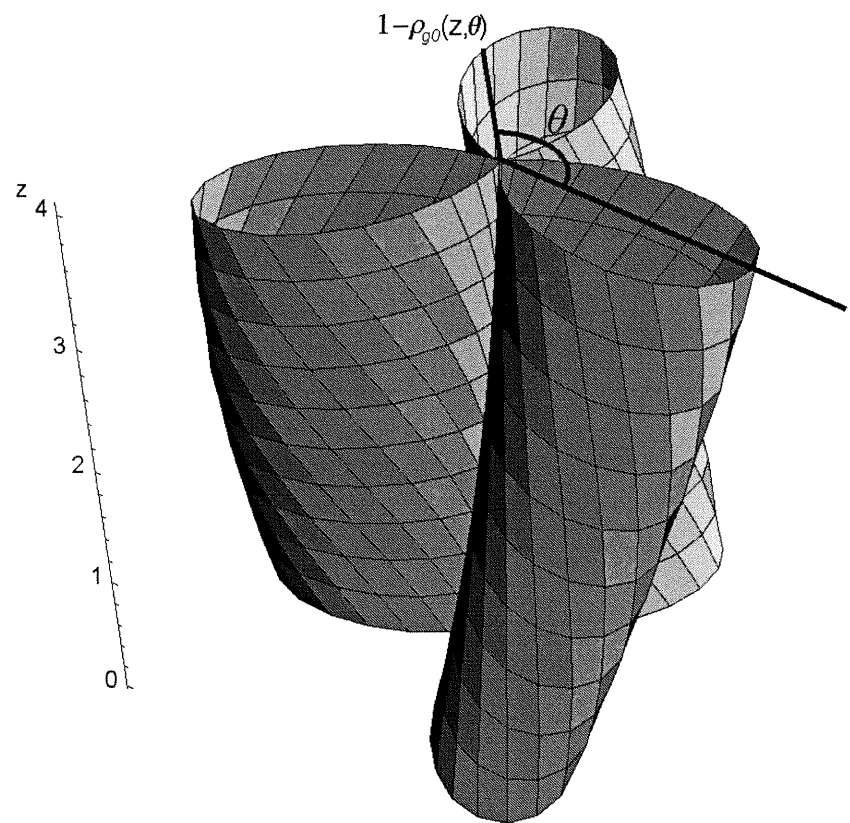


Figure 3

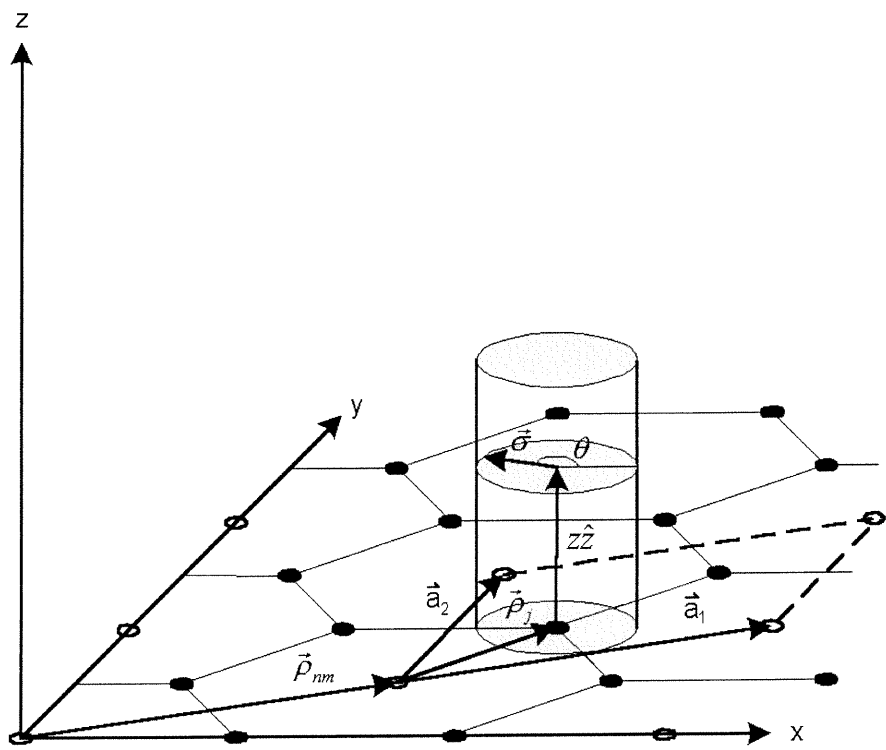


Figure 4

CONCLUSION

Les calculs présentés dans ce travail ont été réalisés à partir d'un modèle de cristal liquide en colonnes au sein duquel les molécules présentent un ordre positionnel et un ordre orientationnel. Ce dernier se traduit, dans notre modèle, par une onde de densité hélicoïdale le long des colonnes qui est incommensurable par rapport à la position des molécules. Un tel modèle se distingue de ceux présentés jusqu'ici dans la littérature par le type d'ordre qui se développe au sein des colonnes. En effet, l'hypothèse d'un quasi-ordre est ici avancée.

De plus, toujours dans le cadre de ce modèle, on a ici séparé la densité de matière en deux quantités distinctes, soit la densité "noyau" (*core density*) et la densité de rainure (*groove density*). Bien que cette catégorisation ne puisse se justifier a priori, il est clair que ces deux quantités, au premier ordre, font référence à des degrés de libertés distincts : le déplacement des centres de masse des molécules le long des colonnes et l'orientation de ces mêmes molécules dans un plan perpendiculaire à cette direction. La finalité de ce modèle n'étant pas d'obtenir l'intensité absolue des maxima de Bragg pour la diffusion des rayons X, mais plutôt une expression analytique décrivant le comportement en lois de puissance de ceux-ci dans l'espace réciproque, il est selon nous justifié de recourir à cette procédure.

Les fonctions de corrélation des fluctuations ont un comportement très anisotrope. On remarque effectivement que si ces quantités possèdent un comportement caractéristique du quasi-ordre le long des colonnes, elles possèdent néanmoins un comportement caractéristique d'un ordre à longue portée dans toute direction perpendiculaire à celle des colonnes. En conséquence, la fonction de corrélation densité-densité "noyau" (*core density-core density correlation function*) est décrite, le long des colonnes, par un comportement en loi de puissance impliquant une série d'exposants qui dépendent des constantes d'élasticité du cristal liquide. La fonction de corrélation densité-densité de

rainure (*groove density-groove density correlation function*) présente également, le long des colonnes, un comportement en loi de puissance. Celui-ci est fonction des hélicités des colonnes. Enfin, toutes les fonctions de corrélation dans le plan perpendiculaire à la direction des colonnes possèdent un comportement caractéristique de l'ordre à longue portée.

Bien que le modèle développé dans le cadre de ce mémoire ne soit pas adéquat afin d'obtenir les intensités relatives des différents maxima de Bragg, il est toutefois raisonnable de l'utiliser pour calculer les effets des fluctuations thermiques sur ces maxima. On remarque que les pics de Bragg dans le plan $\vec{K}_{iz} = 0$ présentent un comportement typique d'un ordre à longue portée. Par ailleurs, les pics de Bragg dans les deux plans $\vec{K}_{iz} = \pm \vec{C}_1$ sont transformés en maxima de Bragg sous l'influence des fluctuations thermiques de la variable positionnelle u_z . L'intensité diffusée présente alors un comportement fortement anisotrope dans l'espace réciproque : elle est caractéristique d'un quasi-ordre dans la direction des colonnes et d'un ordre à longue portée dans le plan perpendiculaire à cette direction.

Quant aux pics de Bragg dus à l'orientation périodique de la densité le long des colonnes, transformés par les fluctuations thermiques orientationnelles en maxima de Bragg, on trouve que leur intensité varie suivant une loi de puissance universelle mais fortement anisotrope. En effet, dans le plan $q_z = 0$, on remarque que l'intensité décroît comme $q_{\perp}^{-1/2}$ tout en étant modulée par une fonction de Bessel d'ordre 3, une particularité que J. D. Watson et F. H. C. Crick ont relevée lors de l'étude de la molécule d'ADN⁸. Par contre, nos calculs indiquent que l'intensité diffusée suivant les colonnes (à $q_{\perp} = 0$) décroît plutôt comme q_z^{-2} .

En résumé, on peut distinguer deux cas particuliers de formation de maxima de Bragg :

1. Au voisinage des vecteurs du réseau réciproque, c'est-à-dire pour $\vec{Q} = \vec{K}_i + \vec{q}_{\perp} + q_z \hat{z}$, on obtient, pour un modèle cristallin (sans fluctuations ther-

⁸J. D. Watson et F. H. C. Crick, Nature **171**, 737 (1953).

miques) et pour le modèle proposé dans ce mémoire (avec fluctuations thermiques), les expressions suivantes pour $I_{cc}(\vec{Q})$:

Position	Modèle cristallin	Modèle proposé
$q_z = 0$	$I_{cc} \propto \sum_i \frac{b_{K_i}^2}{q_\perp^2}$	$I_{cc} \propto \sum_i b_{K_i}^2 \frac{1}{q_\perp^{4-2X(K_i)}}$ (à $K_{iz} = \pm C_1$)
		$I_{cc} \propto \sum_i \frac{b_{K_i}^2}{q_\perp^2}$ (à $K_{iz} = 0$)
$q_\perp = 0$	$I_{cc} \propto \frac{1}{q_z^2}$	$I_{cc} \propto \frac{1}{q_z^2}$

2. Au voisinage des positions des maxima de Bragg dus à l'orientation périodique de densité, c'est-à-dire pour $\vec{Q} = \vec{K}_{hk} + \vec{q}_\perp \pm 3\omega\hat{z} + q_z\hat{z}$, on obtient pour les mêmes modèles, les expressions suivantes pour $I_{gg}(\vec{Q})$:

Position	Modèle cristallin	Modèle proposé
$q_z = 0$	$I_{gg} \propto \frac{J_3^2(K_{hk}R_0)}{q_\perp^2}$ $\times \{3 + 2 \cos[\vec{q}_\perp \cdot (\vec{\rho}_2 - \vec{\rho}_1)]\}$	$I_{gg} \propto \frac{J_3^2(K_{hk}R_0)}{\sqrt{q_\perp}}$ $\times \{3 + 2 \cos[\vec{q}_\perp \cdot (\vec{\rho}_2 - \vec{\rho}_1)]\}$
$q_\perp = 0$	$I_{gg} \propto \frac{1}{q_z^2}$	$I_{gg} \propto \frac{1}{q_z^2}$

Les comportements de l'intensité diffusée au voisinage des maxima de Bragg nous amènent à suggérer que des mesures de diffusion de rayons X à haute intensité et haute résolution devraient être menées afin de vérifier la présence d'un quasi-ordre au sein d'un cristal liquide en colonnes doté d'un ordre orientationnel.

ANNEXE : Définition des constantes d'élasticité et de courbure

Les constantes d'élasticité et de courbure introduites dans la section III de notre article proviennent du développement de l'énergie libre du cristal liquide en colonnes qu'ont réalisé A. Caillé et M. Hébert⁹. En effet, ils ont montré que la densité d'énergie élastique orientationnelle de ce type de cristal liquide, incluant le couplage avec les degrés de liberté positionnels, s'écrit :

$$\begin{aligned}\varepsilon_0(\vec{r}) = & \frac{1}{2}A_1[\varphi_x^2 + \varphi_y^2] + \frac{1}{2}A_2\varphi_z^2 + K_1[\varphi_{xx} + \varphi_{yy}]^2 \\ & + K_2[(\varphi_{xx} - \varphi_{yy})^2 + 4\varphi_{xy}^2] \\ & + B_1[(\epsilon_{xx} + \epsilon_{yy})\varphi_z] + B_2[\epsilon_{xz}\varphi_x + \epsilon_{yz}\varphi_y].\end{aligned}\quad (\text{A1})$$

Les mêmes conventions sont utilisées dans cette expression que dans notre article : $\varphi = \varphi(\vec{r})$ est la variable angulaire décrivant une rotation, dans le plan perpendiculaire aux colonnes, par rapport à la configuration d'équilibre du système. L'axe z est défini parallèle à la direction des colonnes, tandis que le plan xy est perpendiculaire à celle-ci. φ_α est une notation abrégée de $\partial\varphi/\partial x_\alpha$ où $\alpha = x, y$, ou z . De même, $\varphi_{\alpha\beta}$ est une notation abrégée des dérivées secondes. $\epsilon_{\alpha\beta}$ représente les éléments du tenseur de déformation pour les degrés de liberté positionnels. Les termes affectés des coefficients K_1 et K_2 sont les termes de courbure qui comptent parmi les degrés de liberté orientationnels. Les différents paramètres apparaissant dans (A1) ont été calculés¹⁰ à partir d'un hamiltonien microscopique¹¹ et sont apparus comme les termes dominants dans le couplage des degrés de liberté positionnels et orientationnels. À l'expression (A1) est ajoutée la densité d'énergie élastique

⁹A. Caillé et M. Hébert, Phys. Rev. E **54**, R4544 (1996)

¹⁰A. Caillé et M. Hébert, à paraître.

¹¹M. L. Plumer, A. Caillé et O. Heinonen, Phys. Rev. B **47**, 8479 (1993) ; M. Hébert et A. Caillé, Phys. Rev. E **53**, 1714 (1996)

positionnelle d'un cristal de symétrie uniaxiale¹² :

$$\begin{aligned}\varepsilon_e(\vec{r}) = & \frac{1}{2}C_1\epsilon_{zz}^2 + \frac{1}{2}C_2[\epsilon_{xx} + \epsilon_{yy}]^2 + \frac{1}{2}C_3[(\epsilon_{xx} - \epsilon_{yy})^2 + 4\epsilon_{xy}^2] \\ & + \frac{1}{2}C_4[\epsilon_{zz}(\epsilon_{xx} + \epsilon_{yy})] + \frac{1}{2}C_5[\epsilon_{xz}^2 + \epsilon_{yz}^2],\end{aligned}\quad (\text{A2})$$

où les C_i représentent les diverses constantes d'élasticité du système. Ceci met en relief le fait que C_5 est la constante élastique de déformation associée aux déplacements des colonnes les unes par rapport aux autres dans la direction perpendiculaire au plan (la direction \hat{z}).

Tel que l'ont décrit A. Caillé et M. Hébert¹³, l'énergie élastique totale dans l'espace de Fourier s'écrit, à la suite de deux diagonalisations successives, comme :

$$\begin{aligned}E = & \frac{1}{2(2\pi)^3} \int d^3q \left\{ \left[g_1 - \frac{\gamma^2}{4g_2} \right] |u_z(\vec{q})|^2 + g_2 |u'_{q\perp}(\vec{q})|^2 \right. \\ & \left. + \left[\frac{1}{4}C_5q_z^2 + C_3q_\perp^2 \right] |u_\theta(\vec{q})|^2 + f|\Psi(\vec{q})|^2 \right\},\end{aligned}\quad (\text{A3})$$

avec les définitions suivantes :

$$a(\vec{q}) = \left(B_1 + \frac{1}{2}B_2 \right) q_z q_\perp,\quad (\text{A4})$$

$$b(\vec{q}) = \frac{1}{2}B_2 q_\perp^2,\quad (\text{A5})$$

$$f(\vec{q}) = A_1 q_\perp^2 + A_2 q_z^2 + (K_1 + K_2) q_\perp^4,\quad (\text{A6})$$

$$\gamma(\vec{q}) = \left(C_4 + \frac{1}{2}C_5 \right) q_z q_\perp - \frac{ab}{2f},\quad (\text{A7})$$

$$g_1(\vec{q}) = C_1 q_z^2 + \frac{1}{4}C_5 q_\perp^2 - \frac{b^2}{4f},\quad (\text{A8})$$

et

$$g_2(\vec{q}) = (C_2 + C_3) q_\perp^2 + \frac{1}{4}C_5 q_z^2 - \frac{a^2}{4f}.\quad (\text{A9})$$

¹²L. Landau et L. Lifchitz, *Théorie de l'élasticité*, Éditions MIR, Moscou (1967)

¹³A. Caillé et M. Hébert, Phys. Rev. E **54**, R4544 (1996)

CONTRIBUTION DE L'AUTEUR À L'ARTICLE

J'ai d'abord élaboré différents modèles du cristal liquide en colonnes étudié. Par la suite, en m'a aidant de diverses évaluations numériques, j'ai effectué analytiquement les calculs des fonctions de corrélation des fluctuations positionnelles et orientationnelles locales et à grande distance, puis les calculs de la fonction de corrélation densité-densité, et enfin les calculs de l'intensité des rayons X diffusés présentés dans cet article. J'ai rédigé les sections II à V de celui-ci, de même que l'annexe qui décrit les détails des calculs. Enfin, j'ai réalisé les figures apparaissant dans l'article.

REMERCIEMENTS

Je tiens d'abord à remercier Annie, pour sa compréhension et son soutien, de même que toute ma famille, et tout spécialement ma mère, Raymonde, sans qui ce projet n'aurait pu être réalisé. Je vous dédie ce travail.

Ensuite, je souhaite sincèrement remercier mon directeur de recherches, M. Alain Caillé, pour sa grande rigueur intellectuelle, sa bonne humeur, son encadrement, sa disponibilité, son grand respect, son dynamisme et sa générosité. J'ai appris énormément en travaillant avec lui, et il restera à jamais pour moi un modèle d'homme de sciences et d'action.

Je remercie également mes amis de longue date, Jean-François, Dominic et Amik, pour leur aide et leurs encouragements. Merci à mes compagnes et compagnons d'étude de Sherbrooke, Guillaume, Alexandre, Hugues, Benoît, Marjorie, David, Étienne et Marie-Josée, de même qu'à ceux et celles de Montréal, Anna, Noä-Mathieu, Dominique et Gwendoline.

Enfin, je tiens à remercier Louis Lemay, Louise Lafortune et Joëlle Casamajou pour leur support administratif, de même que Francine Senez et Michèle Grenier-Desnoyers pour leurs coups de main documentaires toujours ponctués d'un sourire.